Investigation into Mechanical and Tribological Behaviour of Hollow Glass Microsphere (HGM) Reinforced Epoxy Composite

A Thesis Submitted to

National Institute of Technology, Rourkela

In Partial fulfilment of the requirement for the degree of

Master of Technology

in

Mechanical Engineering

(Specialisation-Machine Design and Analysis)

By

Gaurav Kumar Garg

(Roll No. 213ME1377)

Department of Mechanical Engineering

National Institute of Technology

Rourkela-769008 (India)

May-2015

Investigation into Mechanical and Tribological Behaviour of Hollow Glass Microsphere (HGM) Reinforced Epoxy Composite

A Thesis Submitted to

National Institute of Technology, Rourkela

In Partial fulfilment of the requirement for the degree of

Master of Technology

in

Mechanical Engineering

(Specialisation-Machine Design and Analysis)

By

Gaurav Kumar Garg

(Roll No. 213ME1377)

Under the guidance of

Prof. S. K. Acharya

Department of Mechanical Engineering

National Institute of Technology

Rourkela-769008 (India)

May-2015

National Institute of Technology

Rourkela-769008 (Orissa), INDIA

CERTIFICATE

This is to certify that the thesis entitled "**INVESTIGATION INTO MECHANICAL AND TRIBOLOGICAL PROPERTIES OF HOLLOW GLASS MICROSPHERE (HGM) REINFORCED EPOXY COMPOSITE"** submitted to the National Institute of Technology, Rourkela by Gaurav Kumar Garg Roll No. 213ME1377 for the award of the Master of Technology in Mechanical Engineering with specialization in Machine Design and Analysis is a record of bonafide research work carried out by him under my supervision and guidance. The results presented in this thesis has not been, to the best of my knowledge, submitted to any other University or Institute for the award of any degree or diploma.

The thesis, in my opinion, has reached the standards fulfilling the requirement for the award of Master of Technology in accordance with regulations of the Institute.

Place: Rourkela **(Prof. S. K. Acharya)**

Date: 26th May, 2015 **Department of Mechanical Engineering**

NIT Rourkela

ACKNOWLEDGEMENT

It is a great pleasure to express my gratitude and indebtedness to my supervisor Prof. S. K. Acharya for his guidance, encouragement, moral support and affection through the course of my work.

I am also grateful to Prof. Sunil Kumar Sarangi, Director of NIT Rourkela who took keen interest in the work. My special thanks to Prof. S.S. Mahapatra, Head of Mechanical Engineering Department, for providing all kind of necessary facilities in the department to carry out the experiment.

Besides my advisors, I would like to thank Mrs. Shakuntala Ojha, Mrs. Niharika Mohanta , Ms. Soma Dalbehera and Mrs.Tanu shree berra for constant source of inspiration and ever-cooperating attitude which empowered me in working all the initial surveys, experiments and also to expel this thesis in the present form.

This work is also the outcome of the blessing, guidance and support of my father Mr. Rajendra Prasad Garg & mother Mrs. Vimla Devi. This work could have been a distant dream if I did not get the moral encouragement and help from them. This thesis is the outcome of the sincere prayers and dedicated support of my family. And at last I am extremely thankful to all my friends for their motivation and inspiration during this project work

Date: - 26th May, 2015 **(Gaurav Kumar Garg)**

ABSTRACT

In the present work hollow glass microspheres (HGMs) filled epoxy composite with filler content from 0 to 20 wt. % were prepared in order to improve the abrasive wear and mechanical properties of epoxy. Tensile strength and impact strength were determined experimentally. Abrasive wear test was conducted using pin-on-disc wear tester. Composites having 0, 10, 15, and 20 weight fraction of HGM filled epoxy have been prepared in the laboratory by using a self-designed mould. All the experiments were conducted as per ASTM standard. It was found that as the reinforcement (HGM) increases from 0 to 20 wt. % the wear resistance as well as mechanical properties of composite increases. The enhancement in these properties is related to strong bonding between the HGM and epoxy which might have happened due to formation of an interphase between the HGM and epoxy-matrix. SEM (scanned electron microscope) studies were also carried out to know the fracture behaviour of the composite.

Keywords: **HGM, Pin-on-Disc, Interphase, SEM**

CONTENTS

List of Tables

List of Figures

NOMENCLATURE

F	Load (N)
PMCs	Polymer Matrix Composites
ρ	Density of the target material (gm / cm^3)
ρ_f	Density of filler (gm / cm^3)
ρ_m	Density of Matrix (gm / cm^3)
ρ_{th}	Theoritical Density (gm / cm^3)
ρ_{act}	Actual Density (gm / cm^3)
Δm	Weight loss (gm)
SD	Sliding Distance (m)
W_r	Abrasive wear rate (m^3/m)
W_s	Specific wear rate (m^3/Nm)
W_v	Volumetric wear rate (m^3/sec)
gm	gram

CHAPTER 1

INTRODUCTION

INTRODUCTION

1.1 BACKGROUND:

Framework is frequently marked by the materials and technology that indicate human potential and brainpower. Cyclic work on the material was started in stone period which cause advancement to the Copper, Iron, Steel, Aluminium and Alloy ages, as modernisation in processing, melting took place and science made all these viable to proceed towards detecting more beneficial materials feasible.

Composites are the material made from two or more integral materials with remarkable dissimilar substantial or artificial features, which on joining produced a material having different properties from original constituents. Composites materials can be a single phase or polyphase materials which present a meaningful section of features of both phases it means by joining their features requisite properties can be obtained.

The spectacle materials Composites having low mass to high strength ratio, inflexible and delicate characteristics has swapped most of the metal and alloys in modern times. In current years, polymers and their composites are rapidly substituting the traditional materials in many engineering and systematic implications. Traditional materials have only some finite properties with respect to combination of excessive specific modulus, specific strength and low density etc. These materials have been used in several engineering areas beginning from space craft implementation to industrial unit consumptions due to leading specific strength, leading modulus, low density and improved durability [1]. In aircraft industries where strong, feather, noncorrodible and non-breakable materials are needed and to meet alike specific requirements the composites have to be manufactured.

Being featherweight, while they are the most appropriate materials for weight delicate operations, their expensiveness limited their usage in common implementation. Use of economical, simply achievable fillers is therefore useful to upgrade the properties and to minimize the cost of components [2]. Compact granulated fillers including ceramic or metal bits are being used these days to upgrade wear resistive properties of polymers [3].The injection of such particulates into polymers for commercialized use is especially concentrate at the minimizing price and enhancement of stiffness [4]. Many scholars [5-8] have described that the abrading resistance of polymers upgraded by the inclusions of fillers.

1.2 Types of composites:

According to character of the matrix and filler material the composites can be categorised as follows [9]

- **Particulate reinforced Composites**
    - Big or Large Particulate
    - Dispersion strengthed
- **Fibre reinforced Composites**
    - Continuous
    - Discontinuous
- **Structural Composites**
    - Laminates

1.2.1 Particulate reinforced Composites:

Particle composites contain particles of one material diffuse in a matrix of a second material. Generally the shape of particles is spherical, ellipsoidal, polyhedral, or asymmetrical in shape. In

this the particle is reinforced in the matrix which carry the maximum load whereas the purpose of the reinforcement is to intercept the disorderness in the matrix due to which the plastic distortion is difficult to occur which cause enhancement in hardness as well as tensile strength thus inclusion of fillers refine the properties. Large bits composite is a kind of particle-reinforced composite wherein the synergy of particle matrix cannot be considered on an atomic or molecular stage. The level of augmentation or upgradation of mechanical action controlled by strong bonding at the matrix-particle combination. The size of particle for dispersion-strengthened composites, are generally minor with diameters between 0.01 - 0.1 µm (10 - 100nm).

1.2.2 Fibre reinforced composites:

In fibre reinforced composites the diffused part is in fibre shape, generally they are used where excessive stiffness and strength is necessary as compared to their weight. The fibre's length is the essential variable influencing the features of such composites. The placement and clustering of the fibre also affects the characteristics.

1.2.3 Structural (Laminate) composites:

Laminar or Laminates composite material comes under the category of structural composites. These types of composite materials are composed of layer of material held together by suitable matrix. These types of composite materials have specific properties due to different layers of composite material due to which they are able to perform a specific function. Sandwich structures are the main type of laminar composite.

1.3 Types of composites according to class of matrix

- Metal or Ingot matrix composites
- Pottery or Ceramic matrix composites
- Organic or Polymer matrix composites

1.3.1 Metal or Ingot matrix composites (MMC):

It is a composite material in which there are at least two ingredients, one exist in the form of metal compulsory and the other can be a different ingot or an additional material such as clay or porcelain compound. The filler material causes outstanding changes in working features of the metal and maximum characteristics as abrading resilience, creep resilience refined. Due to these properties it has been used in the field of aerospace such as in the rocket and space shuttle, drilling tools, automotive disc brakes, structural parts etc.

1.3.2 Ceramic or Pottery matrix composites:

In this type of composite pottery or clay or ceramic behave as phase of matrix therefore it is called as clay or ceramic matrix composite. They have excessive hardness and long-lasting in contrast to traditional ceramics while maintaining the basic features such as tenuity, idleness to synthetic response and higher- heat resistance.

1.3.2 Organic or Polymer matrix composites:

In this research work the composite used is polymer matrix composites. In organic matrix composite the polymer is used as a matrix. Polymer is an organic or synthetically fabricated chemical matter containing substantial molecules of numerous classes. Polymers are fabricated by monomers which form a long chain of compound and the process is called polymerisation.

Polymers have light weight and high strength to weight ratio than others; it also has high abrading resilience, due to these features they are used in flying machine and vehicle industries.

1.4 Types of composites according to character of polymer

1.4.1 Thermoset (thermosetting) Polymer matrix composites:

A thermosetting polymer which is also called thermoset is a petroleum component which irreparable restore. The healing can be produce by high temperature, normally greater than 200 °C (392 °F), using a synthetic process, or appropriate illumination. Thermoset matrix are generally liquids or mouldable prior to healing and are used as sealant or adhesive. Due to consequences of that they maintain their bond formation after polymerisation. Example: polyester, Bakelite, polyurethane, and polyepoxides (epoxy) etc.

1.4.2 Thermo softening (or plastic) polymer matrix composites:

This is a plastic material, commonly a polymer, which become mouldable beyond a certain temperature and after cooling they become solid and preserve their shape. They comprise of polymers that have low molecular weight and inadequate bond strength Because of these problems thermoset polymers are better desirable in industry because they are simple during processing and they have low cost contrast to thermo softening polymers. Examples: acrylic, nylon, polypropene, polythene, polycarbonates.

1.5 Benefits of using polymer matrix composites:

(i) Polymer matrix composite has more tensile strength and stiffness

(ii) High abrading resistance

(iii) Cost is low compared to traditional material

1.6 Drawback of polymer matrix composites:

(i) Low thermal resistance

(ii) Distinguished thermal expansion coefficient

1.7 SCIENCE OF WEAR:

Wear is associated with different surface interaction and especially the displacement and distortion of material on a work surface due to mechanical operation of the facing surface. Wear is among the number of operation which takes place when the working surfaces of engineering parts are loaded simultaneously and are treated with sliding, rolling and impact movement [10]. Generally wear arises through surface interactions at during relative motion, material having harder surface may remove the loose particle from softer surface. The wear map offered by Lim and Ashby [11] is very much helpful to determine the wear mechanism in different sliding states moreover as the expected rates of wear. Scientists have evolved many theories in which Physical and Mechanical properties of the materials are considered. The volume of substance decaying over unit slide length was determined by Holm in 1940[12] from the atomic structure of wear. The fatigue theory of wear was evolved by Kragelski [13] in 1957.evolved.This theory has been widely accepted by scientist and researchers of various countries. Owing to the asperities in real bodies, their meshing in sliding is different, and merging takes place at separate position which taken in conjunction from the existent contact area. As per energy theory of wear which was developed by Fleischer [14] in 1973 the detachment of wear particles needed that a definite volume of material gathers a specific condemned reserve of internal energy. In all theories the prime factor is friction.

1.8 CLASSIFICATION OF WEAR

Some common types of wear are classified as

- Surface fatigue wear
- Corrosive Wear
- Rubbing or Grinding or Abrasive wear
- Wear Adherent or adhesive wear
- Erosion wear

1.8.1 Surface fatigue Wear:

Wear occurs due to fracture which emerge due to fatigue of material is called surface fatigue wear. In this type of wear surface of material diminished by repeated loading.

1.8.2 Corrosive Wear:

The decline of exposed material surface due to effects of ambient air, acerbic or acids and some volatile substances like gases etc. is known as corrosive wear. Corrosion generates cavity and aperture and after some time it may disperse parts of the metals.

1.8.3 Abrasive Wear:

Abrasive wear will take place when there is a relative sliding motion between hard and soft surfaces. Due to this loss of material from softer surface occur. Two body abrasions wear takes place when hard or solid grits detach some particles from facing surface.

If the wear is occur due to a hard or solid grit confined between the abrading surfaces then it is known as three body abrasion wear.

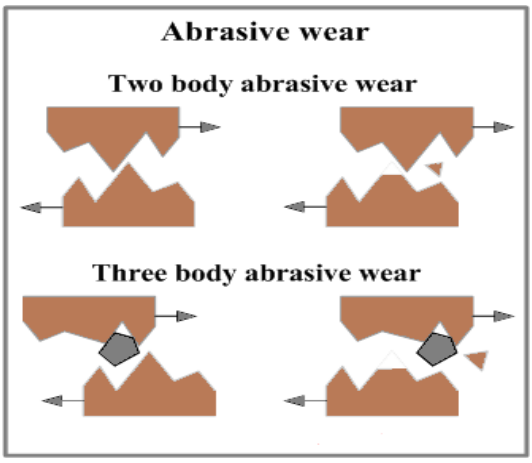

Fig.1.1 Schematic representations of Abrasion wear

1.8.4 Adhesive Wear:

Adhesive wear takes place when there is a localized bonding between two solid surfaces which cause undesired shifting and addition of wear scrap from one surface to another.

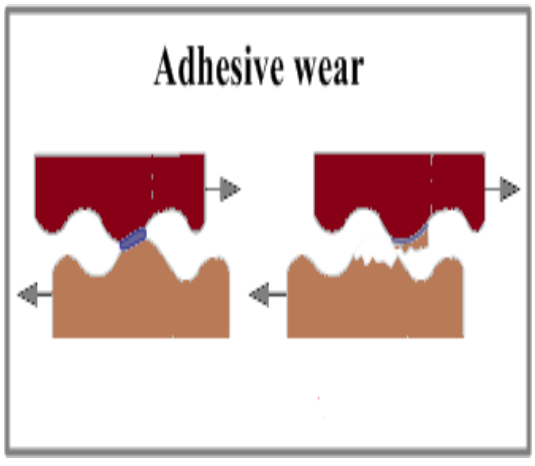

Fig.1.2 Schematic representations of Adhesive wear

1.8.5 Erosion wear:

This type of wear occurred due to impact of solid, liquid or gaseous atoms or molecules or particles contrast to the surface of a body.

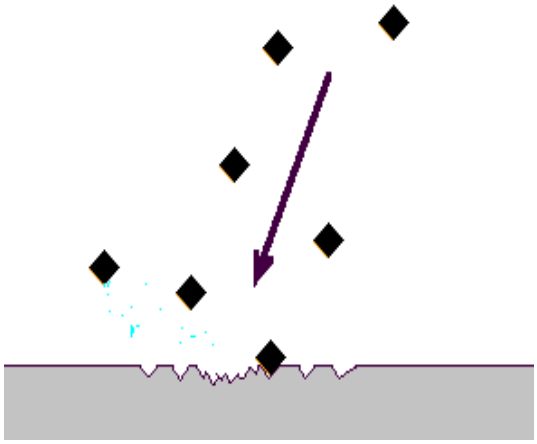

Fig.1.3 Schematic representations of Erosion wear

1.9 Introduction to Polymer composite with Hollow Glass Microsphere (HGM):

1.9.1 Introduction to Hollow Glass Microsphere (HGM):

Hollow glass microspheres (HGMs) are solid spherical particles contain inert gas in inside portion and stiff glass at outer portion. Sometime HGM is also called hollow glass bead or glass bubbles or microballoons. Syntactic foam is an useful form of HGMs filled polymer composites. HGM can be produced by inserting an inactive gas, such as argon into a constant stream of melted glass to create discrete microspheres. The Hollow glass beads are formed by left-over or unused material in coal depending power plants. Due to this, product commonly called as ‘cenosphere’ and conveys aluminosilicate chemistry. Small hollow glass beads are produced by melting of silica in the coal which finally rises up in the chimneystack and spread. Glass beads or

spheres in the form of slag are pumped in a water mixture to the resident ash dam. Hollow particles float on the surface of the dams while some particles which do not become hollow go down in the ash dam. It has feather structure, enormous specific area and economical, low dielectric constant, even flexibility and high corrosion resistance. The delicate microballoons are chemically strong, inflammable, and unyielded and have excellent water resistance. It can be used in coatings, putty, artificial stones etc. It can be used for emulsion explosives. Due to its low density it can be used in oil and gas extraction industries as drilling fluid. The current applications of syntactic foam include remotely and autonomous controlled underwater applications, deep sea inspection, ship hulls, jet and helicopter parts, detector apparent material, audio depletion materials, sporting goods such as bowling ball, tennis racket, soccer balls. Microballoons made of superior optical glasses use in the area of visual resonators.

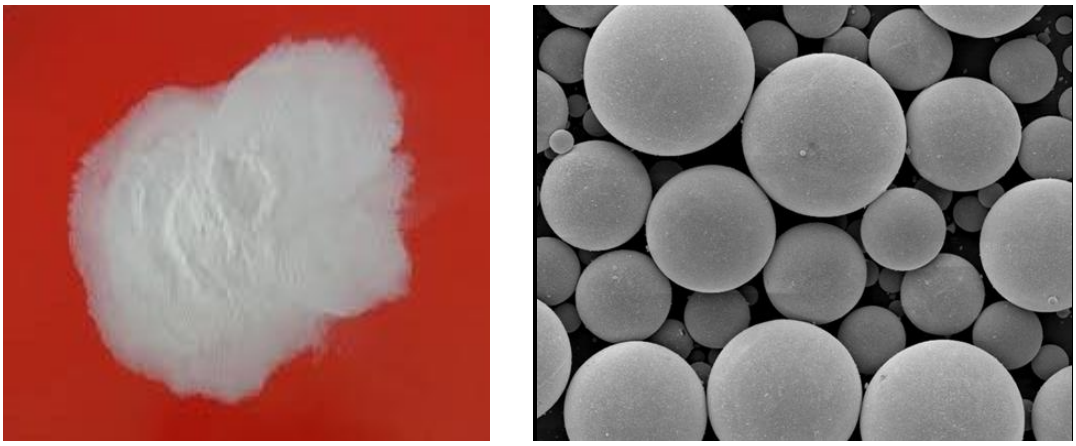

(a) (b)

Fig.1.4 (a) Schematic presentation of Hollow glass microsphere (b) Microscopic view of Hollow glass microspheres particles

1.9.2 Introduction of Epoxy as a polymer matrix:

The main feature of epoxy resin is its low molecular weight with low contraction. However the cost of epoxy resin is higher than other polymer resins. Epoxy resin made by reaction of epichlorohydrin with polyfunctional amine in presence of a strong base. The most commercially available epoxy is diglycidyl ether of bisphenol-A (DGEBA).

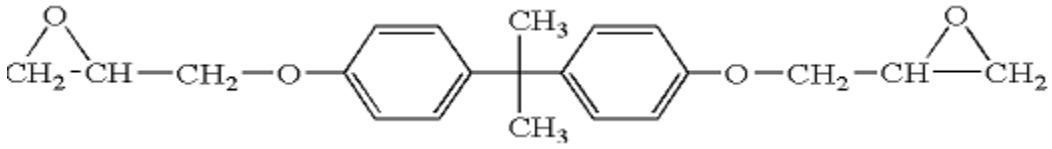

Fig.1.5 Chemical structure of diglycidyl ether of bisphenol-A (DGEBA)

1.7 DEMONSTRATION OF RESEARCH TOPIC:

Ceramic are used as a filler material in polymer matrix during previous two decades due to increasing their application in cladding, electronic wrapping and dental recuperation and it emerged as a subject of vast analysis. Sizes of the particles are in micron. Silicon Carbide, Boron Carbide, Aluminium oxide are used as filler material. The objective of present testing work is to investigate the possibility of Hollow Glass microsphere (HGM) as a filler material in epoxy matrix and to explore its effects on mechanical and tribological properties of resulting composites. HGM filled epoxy composites on the basis of their microsphere content can be categorised in to two forms, one is microsphere modified resin if the content of microsphere is low and other is syntactic foam if the content of microsphere is high. In this work effort has been applied by using different proportion of HGM particle to determine a feasible utilization of HGM that can be fruitfully applicable as particulate filler in epoxy resin for evolving high strength and wear resistant composites.

CHAPTER 2

LITERATURE REVIEW

Chapter 2

2.1 Literature Review

For an analysis of the manufacturing process, characteristics and disintegrating action of polymer matrix composites the literature survey is an essential part of thesis. The aim of the literature study is to make available the background data on the matter linked with current research work and thereby to summarize the aim of the research work. Composite materials exhibit around 20% saving over parts made from metals [15]. Due to substantial development of composite materials in the market, problems related to need of cheapest manufacturing methods and possibilities of reuses will have to be finding out [16].

Composite materials consist polymer as a matrix and ceramic as filler known as ceramic filled polymer matrix composites. These types of composite materials have feather structure or light weight, rusting resistance, wear resistance and low weight to strength ratio [9]. Due to these features polymer matrix composite has been successfully used in vehicle and aerodynamics industries. The behaviour of the composite materials are also effected by properties of wear i.e. how the wear arises and what types of wear may arise etc. and the difference between the mechanism of each wear may be examined by inspecting the working area of profile [17].

2.2 Literature survey on Matrix material:

Since it is not enough to say the matrix a dissolve paste in polymer matrix composite, it is the massive substance which reinforced with filler material and is entirely uninterrupted. Matrix material should be selected merely after giving cautious inspection to its chemical affinity with

the filler material, to its capacity to soak the filler or reinforcement, and to its particular properties and operational technique. Polymer matrix can be manufactured at low cost and it can be easily available. The main disadvantages of polymer matrix are its poor strength and low thermal expansion coefficient. Properties of polymer matrix are humiliated by long lasting disclosure to ultraviolet rays. Carbon atoms in the polymer have covalent bond. Polymers are formed by a process of polymerization.

2.3 Literature survey on Hollow Glass microsphere (HGM):

In the present research work HGM is used as a reinforced material. In contrast to previous clay or terracotta or ceramic particles or particulates HGM filled polymer composite has remained a comparatively less investigated area. HGM is also called glass microballoon or syntactic foam.

Ritter J et al. [18] studied that properties of glass beads products such as smooth surface, scattered internal stress, easy manufacturing make it usable in industrial field. Structural properties of the syntactic foams examined by many researchers over precedent 20 years.

Shao-Yun Fu et al. [19] studied that stiffness, strength and toughness of particulate composites are highly effected by the size of particle, bonding between particle and matrix and load on particle. However the stiffness is depending on load on particle rather than sticking of particle and matrix because higher modulus of particle as compared to matrix. Sticking or adhesion regulates the toughness of composite material.

Kinloch A.J. et al. [20] investigate that to raise the mechanical and physical properties of the polymer resins microballoons can be used commercially with thermosets or thermoplastic resins.

Sahu and Broutman et al. [21] investigated the fractural and mechanical behaviour of HGM filled polyester and epoxy resins with different particulate matrices boundary conditions. According to him glass beads are preferred as filler when the properties such as low melting viscosity or isotropy are desired.

Broutman and Mallick et al. [22] studied the fracture, flexural and compressive characteristics of reinforced glass powder having size of particle 15 micron with epoxy as a brittle matrix.

Ravi Kumar et al. [23] observed that compressive strength of syntactic foam for a volumetric fraction of 0-60 % of hollow glass microsphere. According to him the compressive strength of syntactic foam directly decreases with increase in volumetric fraction of hollow glass microsphere. He examined that the compressive strength decrease in linear manner from 105 MPa to 25 MPa.

J.R.M. d'Almeida et al. [24] examined the effect of diameter of glass microsphere on the mechanical performance of glass filled epoxy composite. They found that the thickness of wall of microsphere is not related with their mean size.

S. Basavarajappa et al. [25] studied the sliding wear behaviour of composite having glass epoxy filled with graphite and Si (silicon) particles at several loads, sliding speed and sliding distance. According to him specific wear rate will increase directly increase of sliding velocity. Specific wear rate was more influenced by applied load as compared to sliding velocity and sliding distance.

K.C.Yung et al. [26] investigated the thermal properties of HGM filled epoxy composite with volumetric content of filler in the range of 0-51.4 %. They found the improvement in thermal

expansion coefficient and glass transition temperature with increase in HGM content but lowering of dielectric loss and dielectric constant of composite.

Soo – Jin Park et al. [27] examined the enhancement of mechanical interfacial and dynamic mechanical characteristics of HGM bonded with epoxy matrix. According to him HGM filled epoxy composites have higher free surface energy.

Ho Sung Kim et al. [28] investigated that impact behaviour of composite material can be improve by addition of HGMs content but it will occur at the loss of flexural strength and fracture toughness.

Jingjie Zhang et al. [29] investigated that with increase in content of broken HGMs in silicon rubber matrix thermal conductivity, mechanical characteristics and density will improve.

Xuegang Luo et al. [30] developed the HGM filled poly butylene succinate (PBS) composite. He tested that inclusion of HGM content (5 to 20 wt. %) enhanced the thermal stability, stiffness and viscosity of PBS but decreased the density of composite.

Peifeng Li et al. [31] developed a three dimensional finite element model of cubic representative elementary model (REV) to determine the failure mechanism and elastic behaviour of syntactic foam with different volume proportion of HGM.

Jinhe wang et al. [32] observed the improvement in the mechanical characteristics such as impact strength, flexural modulus and flexural strength of bisphenol a dicyanate ester with inclusion of hollow glass microspheres.

Chang Keun Kim et al. [33] prepared a thermoplastic polyurethane grafted HGM composite which can be used in underwater applications. According to him the tensile strength is directly enhance with enhancement in HGM concentration whereas the density and the swelling proportion decreased on increment of HGM concentration.

P.Li et al. [34] examined the propagation of shear ruptures at higher strain rates through microballoons in syntactic foam which exhibited the macroscopical strain rate reliance of compressive characteristics.

Liang and Li et al. [35, 36] studied the flexural and tensile features of acrylonitrile butadiene styrene (ABS) filled with hollow glass bead and impact and tensile characteristics of Polyvinyl chloride filled with hollow glass bead.

J. A. M. Ferreira et al. [37] observed the uninterrupted reduction in fatigue strength of HGM filled epoxy composites.

CHAPTER 3

MECHANICAL TESTING OF HOLLOW GLASS MICROSPHERE REINFORCED EPOXY COMPOSITE

Chapter 3

3.1 Material used:

Following materials are used in this research work

(i) Ceramic particulate (Hollow Glass Microsphere or HGM)

(ii) Polymer Matrix (Epoxy Resin)

(iii) Hardener

3.1.1 Hollow Glass Microsphere (HGM):

HGM used in this research is white in colour and supplied by 3M India with density 0.15 g/cc (K15). The hollow glass microsphere used in this research is chemically stable soda lime borosilicate glass composition having a thermal stability of 600°C. The microspheres had a wall thickness between 10 and 30µm with particle diameters ranging from 10 to 150µm.

Table 3.1: Chemical composition of borosilicate glass

Components	Wt. % Composition
SiO_2	44.7
Al_2O_3	12.5
B_2O_3	14.1
CaO	26.3
Na_2O	0.6
K_2O	0.7

Table.3.2: Properties of Hollow Glass Microsphere according to 3M

Property	Value
Shape	Hollow, Thin Walled, Unicellular
Composition	Soda-lime borosilicate
Colour	White
True Density	0.15-0.60 g/cm^3
Crush Strength	250-30,000 Psi
Softening Temperature	600 °C
Size	10 – 100 microns

3.1.2 Epoxy Resin:

The epoxy resin used in the current research work is araldite LY556 (bisphinol-A-diglycidyl-ether) which is a part of epoxide group. This type of epoxy resin is supplied by CIBA GUGYE India Limited. It has following good properties:

- Dimensionally stable
- Internal stress is very low
- Outstanding bonding with different materials
- Low contraction and Inactive to atmospheric and chemical effects
- Bio-degradable, odourless, harmless, distasteful
- Better electrical and mechanical properties related to other thermoset plastics

3.1.3 Hardener:

The hardener HY 951with IUPAC name NNO-Bis (2aminoethylethane-1,2diamin) was used in this research with epoxy resin as a matrix in 10:1 ratio. HY 951 is aliphatic amines. Its viscosity is 10-20 MPa at 25°C.

3.2 Experimental Details

3.2.1 Sample Preparation:

In the present work hollow glass microsphere is taken as filler material. For tensile and impact testing the composite material is fabricated by using hand lay-up technique as shown in fig.3.1. A Per-pex sheet mould of dimension 150×60×6 mm^3 was used for fabrication of composite. Calculated amount of epoxy resin and hardener (10:1 ratio) were mixed along with the reinforcement (10, 15 and 20 wt. % HGM) by stirring process. Adequate care has been taken to avoid air entrapment during pouring. After mixing the mixture was decant or poured into prepared mould as shown in fig.3.2. Before pouring the mixture a mould release spray was used at the inner surface of mould for secure and instantaneous release of composite. After pouring pressure was applied from the top and mould was allowed to cool at room temperature for 72 hrs. After 72 hrs. the specimens were taken out of the mould. After removing from mould the specimen as shown in fig.fig.3.3 were cut into different dimensions and stored in air tight container for further experimentation.

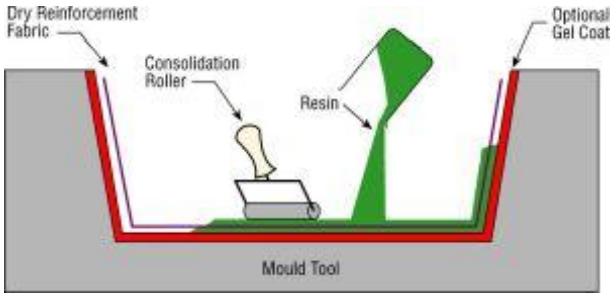

Fig. 3.1: Hand Lay-up set up

Fig. 3.2 mould used for making the composite

Fig.3.3 Specimen after fabrication

3.3 Characterization of Composites

3.3.1 Density Measurement

By using following equation density of composite material determined in terms of volume fraction

$$\rho_{ct} = \frac{W_o}{W_o + \left(W_a - W_b\right)} \qquad \text{..... (1)}$$

Where, ρ_{ct} = specific gravity of the composite, w_o = weight of the sample

w_a = weight of the bottle + kerosene, w_b = w_a + sample,

Density of composite = ρ_{ct} × density of composite. In terms of weight fraction the theoretical density of composite can be determined from formula given by Agarwal and Broutman [32]

$$\rho_{ct} = \frac{1}{\left(\frac{w_f}{\rho_f}\right) + \left(\frac{w_m}{\rho_m}\right)} \quad \text{..... (2)}$$

Where w and ρ are the weight and density correspondingly. The suffix f, m, ct represent the fibre, matrix and composite materials respectively

3.3.2 Void Content

According to ASTM D-2734-70 standard the void content in the composite sample can be determined by using following expression

$$V_v = \frac{\rho_t - \rho_a}{\rho_t} \quad \text{..... (3)}$$

Where, ρ_t = Theoretical Density and ρ_a = Actual Density

3.3.3 XRD (X-Ray Diffraction) Analysis

XRD is an exclusive method to find out the crystallinity (amorphous or crystalline) of composite material, placement of particulates in specimen etc. This analysis is based on diffraction of X-rays. When X-rays incident on the specimen then it create diffracted X-ray then different peaks with different intensity was observed which should fulfil the Bragg's equation i.e. [n $n\lambda = 2d\sin\theta$], where λ is the wavelength of X-ray radiation and θ is the angle of diffraction. The measurement of the intensity and diffraction angle is helpful to find out the crystallinity of

the specimen. In the present work an advance X-ray Cu K-α radiation diffractometer worked at voltage of 30V and current of 20A with wavelength of 0.15418 nm. The range of intensity (2θ) was $20^{\circ} - 80°$. The X-ray diffraction diagram of hollow glass microsphere filled epoxy composite is shown as below

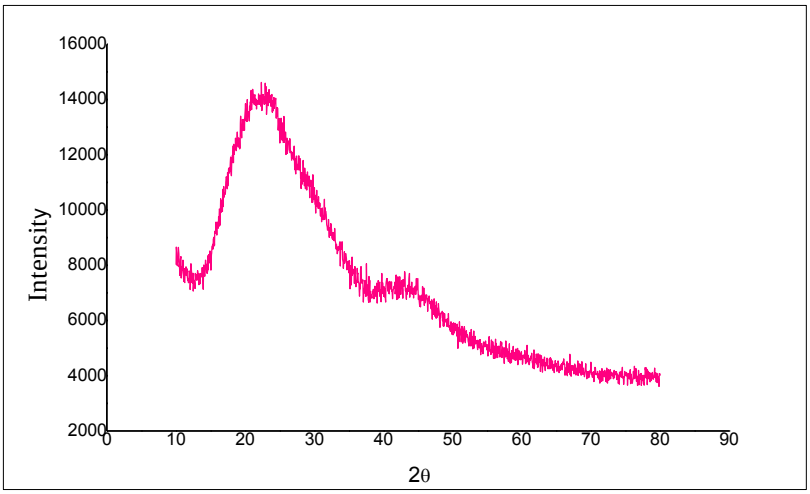

Fig.3.4 Intensity Variation with diffraction angle

From the above figure for each profile crystallinity peak of the material was obtained at approximate $2\theta = 22.9°$ and $43.05°$ at intensity 14593.33 and 7766.62 respectively. Value of crystallinity peak between 22.9° and 43.05° represent the presence of carbon element in the composite. Some zigzag type peaks in figure represent the amorphous structure of HGM filled epoxy composite.

3.4 Testing of Mechanical Properties of Composites

3.4.1 Tensile Test

The tensile test of composite was carried out as per ASTM D 3039-76 standard by using UTM (universal testing machine) INSTRON H10KS. The required dimension (140×15×6 mm^3) of specimen was cut from the composite cast. Normally tensile test is accomplished on a pooch (dog)-bone shaped flat specimen. The gauge length of the tested specimen was 42 mm. During testing the strain rate kept constant and the value of it was 2 mm/min. 5 specimen of composite tested for each test and for examination there average value was taken. The results were examined to determine the tensile strength of the composite specimens.

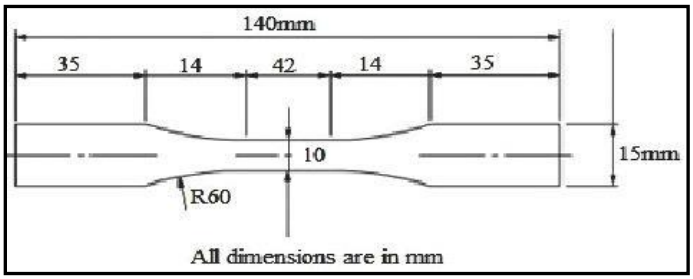

Figure 3.5 Dog bone shape of the tensile testing sample

Figure 3.6 (a) UTM Machine Sample holder (b) UTM Machine Sample Loaded

Table 3.3: Tensile characteristics of HGM filled epoxy composite

Weight % of filler	Tensile Strength of composite (MPa)
Pure Epoxy(0)	14.842
10	15.146
15	17.952
20	20.735

3.4.2 Impact Test

To analyse the toughness behaviour of the composite impact test was conducted. During the test, a large amount of force was exerted on specimen for a very short interval of time. For any material if the value of impact strength is high then the material can absorb the large amount of energy before failure. The value of toughness and the plasticity of material increase with increase of impact energy. Figure 3.7 shows the picture of impact testing machine. During testing a pendulum was released from a certain height to strike the clamped specimen. From dial indicator the corresponding values of impact energy of different specimens were getting directly. The size of the specimen for the impact test was $63.5 \times 12.7 \times 6.2\,\text{mm}^3$. Table 3.2 represent the different values of impact strength under different weight % of filler.

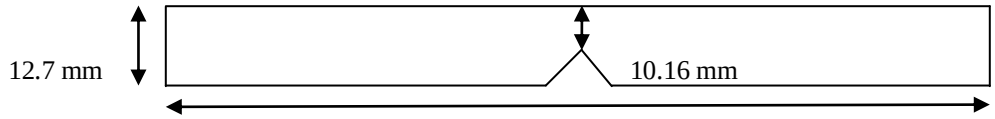

Fig. 3.7: Dimension of impact test specimen

Table 3.4: Impact characteristics of HGM filled epoxy composite

Weight % of filler	Impact Strength of composite (KJ/m^2)
Pure Epoxy(0)	2.31844
10	3.38637
15	4.77803
20	5.67813

Fig. 3.8: Pictographic view of Impact tester

3.5 RESULTS AND DISCUSSION

3.5.1 Effect of filler concentration on tensile strength of composite

The effect of filler content or concentration has been shown in fig. 3.9. It is found that the tensile strength of the composite increase with increase in weight % of filler. When the composite is subjected to normal load then the particulate material act as load carrier and epoxy matrix transfer the stress to the filler uniformly. At higher filler concentration the composite has better tensile strength. In the plot the value of tensile strength is highest for 20 wt. %

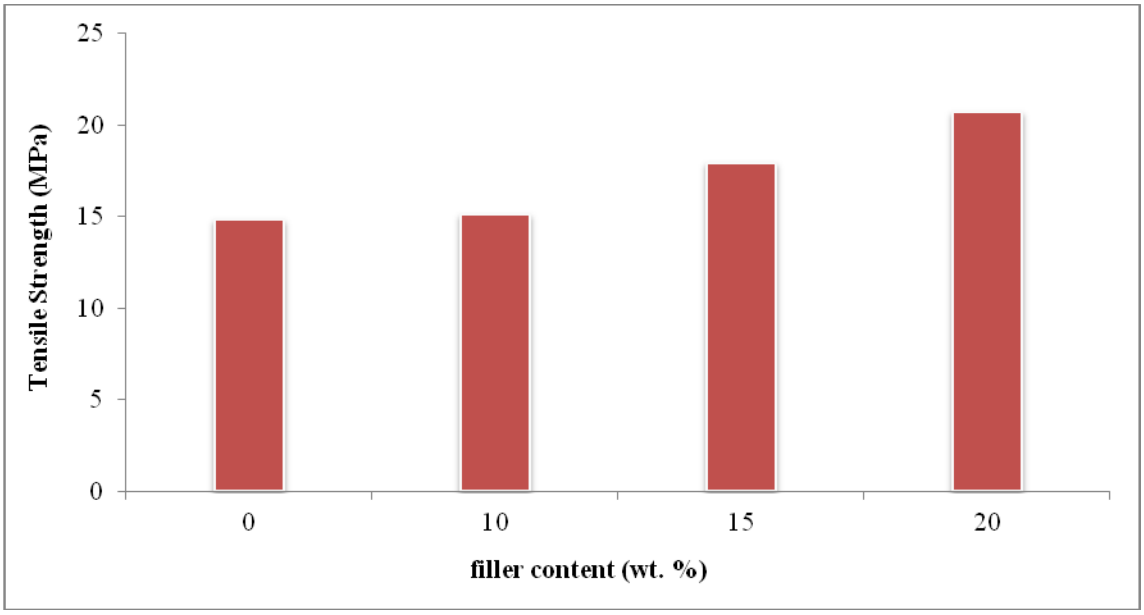

Fig. 3.9: Effect of hollow glass microsphere content on tensile strength of composite

3.5.2 Effect of filler concentration on impact strength of composite

The variation of impact strength with increase in filler content has been shown in fig. 3.10. Improvement in the impact strength of composite has obtained with addition of filler in epoxy resin matrix. Fracture of filler particles, separation of particulate filler are the main reasons

behind fracture of composite during impact loading. Therefore the increase in impact strength occurs due to enhancement in applied energy. In the figure 4.4 filler content with 20 wt. % exhibits higher impact strength. With increase in filler content in composite more energy will be required for weakening of particulate filler matrix bonding.

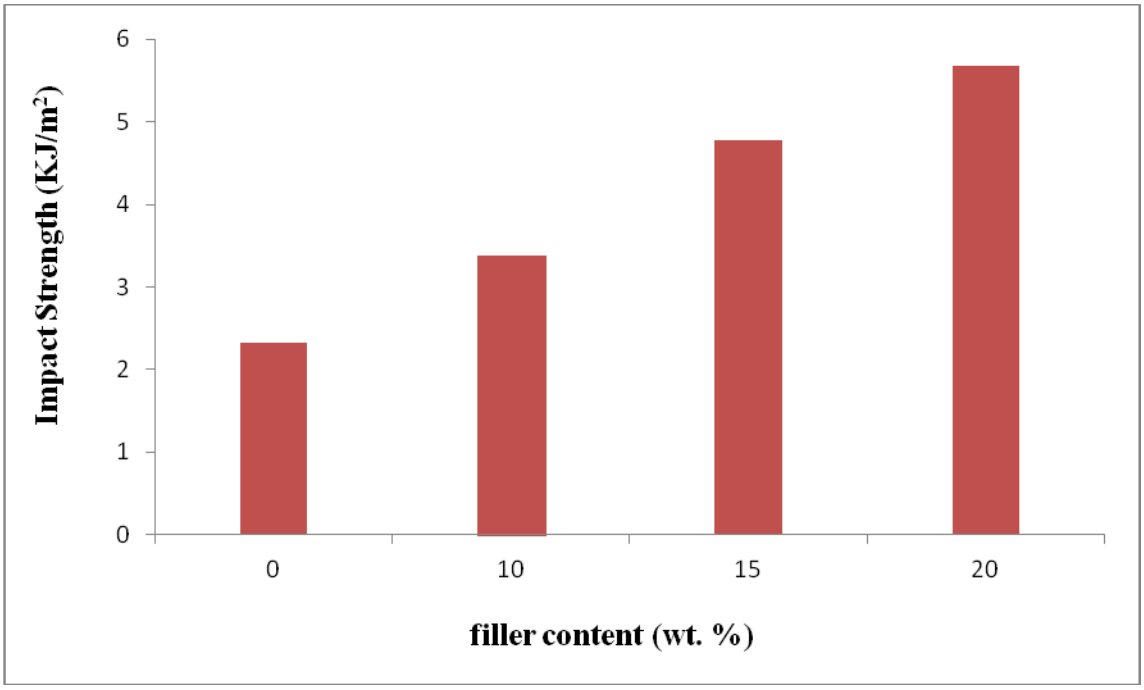

Fig.3.10: Effect of hollow glass microsphere content on impact strength of composite

CHAPTER 4

DRY SLIDING ABRASIVE WEAR TESTING OF HOLLOW GLASS MICROSPHERE (HGM) FILLED EPOXY COMPOSITE

Chapter 4

4.1 INTRODUCTION

Abrasion wear is the most intimidate wear in the industrial field which decline the life span of expensive machine part [55]. In terms of cost this type of wear comprise 63 % of entire cost of wear which occur when a harder surface has relative sliding motion against the softer surface under applied load, it pierces and detach some material from the surface has low hardness which cause cracks in the softer material. Those types of sliding parts are not failed by cracks only but they may also failed by decline of surface due to kneading of softer surfaces against the harder [57]. According to available literature the rate of wear caused by abrasion may vary rapidly at a definite contact loads and sliding velocities. For attaining the development in the wear resistance of polymer matrix composites an extensive consideration of the mechanism of abrasive wear is required. The effects of random variables on the behaviour of abrasive wear of polymer matrix composites can be resolved.

4.2 EXPERIMENTAL DETAILS

4.2.1 Composite fabrication

The particulate in a requisite amount (10, 15 and 20 wt. %) were mixed with epoxy resin along with measured quantity of hardener. Composite specimens in cylindrical (pin) shape were prepared in a steel mould as shown in fig.4.1. The length and diameter of specimen are 55 mm and 10 mm respectively. The mixture of hollow glass microsphere particles and epoxy resin was

poured into the cylindrical cavity of mould. Then two halves of mould as shown in fig.4.2 were fastened or fixed. Proper precaution was taken for squeezing out of mixture for the duration of fabrication of composites. Specimen was solidify in the mould for 24 hours at room temperature. Then prepared samples were taken out from the mould and used for dry sliding abrasive wear test.

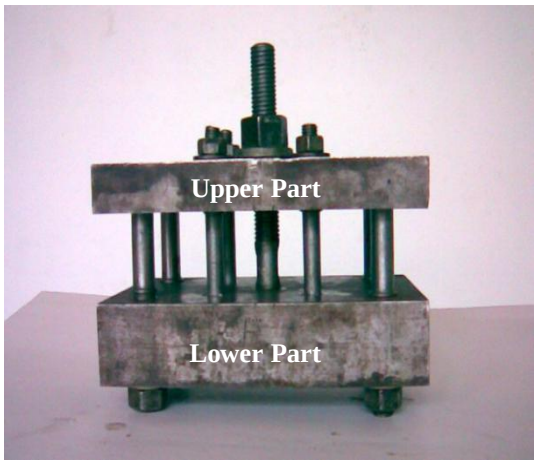

Fig.4.1: Mould used for preparing samples

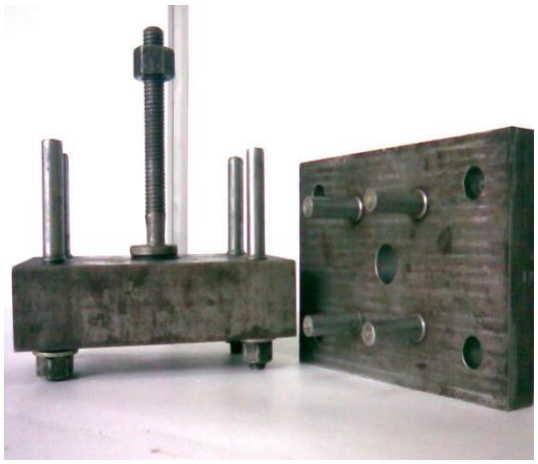

Fig.4.2: Two halves of the mould

Fig.4.3: Fabricated Composite pins

4.2.2 Dry Sliding Wear Test

Dry sliding abrasive wear test was conducted on a pin-on-disc machine according to ASTM G-99 standard which was provided by Magnum Engineers, Bangalore. On a rotating disc (EN 31) whose diameter is 120 mm an abrasive paper of 400 grades (grit-23 µm) has been pasted. The specimen was fixed in a sample holder which was located at a defined track diameter. After each test the diameter of track was changed or we can say that a new and unmarked surface is to be provided for each specimen .Track radius 50 mm was taken for testing and kept unchanging for whole experiment. During testing specimen remain fixed and the disc rotates. By the help of dead weight loading system load was exerted to press the pin against the disc. A control panel was provided in machine to vary the speed of the disc and time period. The total duration for testing of single specimen was 25mins. By calculating the weight of specimen before and after each test the mass loss can be determined. Before and after testing specimen should be cleaned with acetone.

Fig. 4.4: Pin-on-disc machine

Fig.4.5: Fabricated Pin under testing

4.2.3 Calculation of Wear

Wear rate was estimated by measuring the weight loss of the specimen after each test. The weight loss was calculated by taking the weight difference of the sample before and after each test. The weight loss:

$$(\Delta m) = (m_a) - (m_b) \text{ gm} \quad \text{.....(4)}$$

Where, Δm = weight loss in gm, m_a = weight of specimen prior to testing in gm (gram)

m_b = weight of specimen after testing in gm.

Dry sliding abrasive wear rate (W_r) can be determined by using the following formula:

$$W_r = \frac{\Delta m}{\rho \times SD} \quad \text{mm}^3/\text{m} \quad \text{.....(5)}$$

Where, ρ = density of the composite in g/cm^3, SD = sliding distance in meter

Volumetric wear rate (W_v) of the composite which depend upon density (ρ) and the abrading time (t), can be determined using following formula

$$W_v = \frac{\Delta m}{\rho \times t} \quad \text{m}^3/\text{sec} \quad \text{.....(6)}$$

Where, t is the time in which composite has sliding motion with disc

The abrasive wear performance of composite can be classify using the **specific wear rate (**W_s) which is defined as the volume loss of the composite per unit sliding distance and per unit applied load. It can be determined by using following expression

$$W_s = \frac{\Delta m}{\rho \times SD \times F} \text{ m}^3/\text{Nm} \quad \text{.....(7)}$$

Where, Δm = the mass loss in grams,

SD = sliding distance in meter

F = applied normal load in N.

The different values of weight loss, wear rate, volumetric wear rate and specific wear rate under different test condition is listed in Table-4.3 to 4.37.

Coefficient of friction (μ) can be determined by using following equation:

$$\mu = \frac{F_f}{F} \quad \text{..... (8)}$$

Where, F_f is the frictional force in N obtained from control panel directly and F is the applied normal force in N.

Table 4.1: Test Parameter for dry sliding abrasion wear test

Test Parameter	Units	Values
Weight fraction of filler	%	0, 10, 15 and 20
Load (L)	N	5, 10 and 15
Sliding Velocity	m/s	1.047, 1.571 and 2.094
Track Radius (r)	mm	50
Temperature	℃	25

Table 4.2: Density of different samples

Fibre %	Theoretical Density (gm/cm^3)	Actual Density (gm/cm^3)	Void Fraction
0	1.20	1.181	1.583
10	0.706	0.698	1.116
15	0.585	0.579	1.087
20	0.500	0.496	0.810

Table 4.3

Pure Epoxy **Load- 5 N** **Velocity – 1.047 m/s**

m_1 (gm)	m_2 (gm)	Δm (gm)	t (sec)	$SD \times 10^3$ (m)	F_f (N)	μ	$W_r \times 10^{-10}$ (m^3/m)	$W_s \times 10^{-11}$ (m^3/Nm)	$W_v \times 10^{-10}$ (m^3/s)
3.389	3.024	0.365	300	0.314	4.61	0.922	9.84268	19.6854	10.302
3.389	2.796	0.593	600	0.628	4.49	0.898	7.99549	15.9910	8.36861
3.389	2.583	0.806	900	0.942	4.35	0.87	7.24493	14.4899	7.58303
3.389	2.489	0.900	1200	1.256	4.17	0.834	6.0674	12.1348	6.35055
3.389	2.368	1.021	1500	1.570	4.01	0.802	5.503	11.006	5.76348

Table 4.4

Pure Epoxy **Load- 5 N** **Velocity – 1.571 m/s**

m_1 (gm)	m_2 (gm)	Δm (gm)	t (sec)	$SD \times 10^3$ (m)	F_f (N)	μ	$W_r \times 10^{-10}$ (m^3/m)	$W_s \times 10^{-11}$ (m^3/Nm)	$W_v \times 10^{-10}$ (m^3/s)
2.618	1.951	0.667	300	0.471	4.6	0.92	11.99001	23.982	18.8259
2.618	1.623	0.995	600	0.942	4.56	0.912	8.9438	17.8876	14.0418
2.618	1.437	1.181	900	1.413	4.45	0.89	7.07714	14.1543	11.1111
2.618	1.407	1.211	1200	1.884	4.325	0.865	5.44269	10.8854	8.54502
2.618	1.397	1.221	1500	2.355	3.971	0.792	4.3901	8.78021	6.89246

Table 4.5

Pure Epoxy **Load- 5 N** **Velocity – 2.094 m/s**

m_1 (gm)	m_2 (gm)	Δm (gm)	t (sec)	$SD \times 10^3$ (m)	F_f (N)	μ	$W_r \times 10^{-10}$ (m^3/m)	$W_s \times 10^{-11}$ (m^3/Nm)	$W_v \times 10^{-10}$ (m^3/s)
3.191	2.461	0.73	300	0.628	4.6	0.92	9.84366	19.700	20.60610
3.191	1.997	1.194	600	1.256	4.56	0.912	8.05588	16.100	16.86364
3.191	1.556	1.635	900	1.884	4.45	0.89	7.36827	14.700	15.42424
3.191	1.144	2.047	1200	2.512	4.325	0.865	6.88694	13.800	14.42424
3.191	0.763	2.428	1500	3.140	3.471	0.6942	6.57209	13.100	13.75758

Table 4.6

Pure Epoxy **Load- 10 N** **Velocity – 1.047 m/s**

m_1 (gm)	m_2 (gm)	Δm (gm)	t (sec)	$SD \times 10^3$ (m)	F_f (N)	μ	$W_r \times 10^{-10}$ (m^3/m)	$W_s \times 10^{-11}$ (m^3/Nm)	$W_v \times 10^{-10}$ (m^3/s)
3.182	2.737	0.445	300	0.314	9.2	0.92	12.0000	12.0000	12.5600
3.182	2.435	0.747	600	0.628	9.12	0.912	10.0719	10.0719	10.5419
3.182	2.182	1.000	900	0.942	8.9	0.89	8.98875	8.98875	9.40822
3.182	1.937	1.245	1200	1.256	8.65	0.865	8.39324	8.39324	8.78493
3.182	1.707	1.475	1500	1.570	6.942	0.6942	7.94998	7.94998	8.32628

Table 4.7

Pure Epoxy **Load- 10 N** **Velocity – 1.571 m/s**

m_1 (gm)	m_2 (gm)	Δm (gm)	t (sec)	$SD \times 10^3$ (m)	F_f (N)	μ	$W_r \times 10^{-10}$ (m^3/m)	$W_s \times 10^{-11}$ (m^3/Nm)	$W_v \times 10^{-10}$ (m^3/s)
3.625	2.77	0.855	300	0.471	9.2	0.92	15.3708	15.3708	24.1321
3.625	2.448	1.177	600	0.942	9	0.9	10.5798	10.5798	16.6102
3.625	2.208	1.417	900	1.413	8.9	0.89	8.49137	8.49137	13.3315
3.625	2.075	1.55	1200	1.884	8.65	0.865	6.96628	6.96628	10.9371
3.625	1.906	1.719	1500	2.355	6.942	0.6942	6.18066	6.18066	9.70364

Table 4.8

Pure Epoxy **Load- 10 N** **Velocity – 2.094 m/s**

m_1 (gm)	m_2 (gm)	Δm (gm)	t (sec)	$SD \times 10^3$ (m)	F_f (N)	μ	$W_r \times 10^{-10}$ (m^3/m)	$W_s \times 10^{-11}$ (m^3/Nm)	$W_v \times 10^{-10}$ (m^3/s)
2.481	1.243	1.238	300	0.628	9.2	0.92	16.6921	16.6921	34.9421
2.481	0.718	1.763	600	1.256	9.12	0.912	11.8854	11.8854	24.8800
2.481	0.665	1.816	900	1.884	8.9	0.89	8.16178	8.16178	17.0853
2.481	0.582	1.899	1200	2.512	8.65	0.865	6.40111	6.40111	13.3997
2.481	0.483	1.998	1500	3.141	6.942	0.6942	5.38614	5.38614	11.2786

Table 4.9

Pure Epoxy **Load- 15 N** **Velocity – 1.047 m/s**

m_1 (gm)	m_2 (gm)	Δm (gm)	t (sec)	$SD \times 10^3$ (m)	F_f (N)	μ	$W_r \times 10^{-10}$ (m^3/m)	$W_s \times 10^{-11}$ (m^3/Nm)	$W_v \times 10^{-10}$ (m^3/s)
2.445	1.963	0.482	300	0.314	12.045	0.803	12.9977	8.66515	13.6043
2.445	1.652	0.793	600	0.628	10.065	0.671	10.6921	7.12808	11.1911
2.445	1.349	1.096	900	0.942	9.810	0.654	9.85167	6.56778	10.3114
2.445	1.083	1.362	1200	1.256	9.600	0.64	9.18201	6.12134	9.6105
2.445	0.835	1.61	1500	1.571	9.510	0.634	8.6776	5.78507	9.08834

Table 4.10

Pure Epoxy **Load- 15 N** **Velocity – 1.571 m/s**

m_1 (gm)	m_2 (gm)	Δm (gm)	t (sec)	$SD \times 10^3$ (m)	F_f (N)	μ	$W_r \times 10^{-10}$ (m^3/m)	$W_s \times 10^{-11}$ (m^3/Nm)	$W_v \times 10^{-10}$ (m^3/s)
3.392	2.500	0.892	300	0.471	13.800	0.92	16.0359	10.6906	25.1764
3.392	2.064	1.328	600	0.942	13.680	0.912	11.9371	7.95804	18.7412
3.392	1.834	1.558	900	1.413	13.350	0.89	9.33631	6.22421	14.658
3.392	1.406	1.986	1200	1.884	12.225	0.815	8.92583	5.95055	14.0135
3.392	1.385	2.007	1500	2.355	10.413	0.6942	7.21617	4.81078	11.3294

Table 4.11

Pure Epoxy **Load- 15 N** **Velocity – 2.094 m/s**

m_1 (gm)	m_2 (gm)	Δm (gm)	t (sec)	$SD \times 10^3$ (m)	F_f (N)	μ	$W_r \times 10^{-10}$ (m^3/m)	$W_s \times 10^{-11}$ (m^3/Nm)	$W_v \times 10^{-10}$ (m^3/s)
3.309	1.951	1.358	300	0.628	13.800	0.92	18.3101	12.2067	38.3291
3.309	1.531	1.778	600	1.256	13.680	0.912	11.9865	7.99100	25.0917
3.309	1.194	2.115	900	1.884	13.350	0.89	9.50560	6.33707	19.8984
3.309	1.094	2.215	1200	2.512	12.975	0.865	7.46628	4.97752	15.6294
3.309	0.989	2.32	1500	3.141	10.413	0.6942	6.25418	4.16945	13.0962

Table 4.12

Weight Fraction- 10% **Load- 5 N** **Velocities – 1.047 m/s**

m_1 (gm)	m_2 (gm)	Δm (gm)	t (sec)	$SD \times 10^3$ (m)	F_f (N)	μ	$W_r \times 10^{-10}$ (m^3/m)	$W_s \times 10^{-11}$ (m^3/Nm)	$W_v \times 10^{-10}$ (m^3/s)
2.886	2.739	0.147	300	0.314	4.6	0.92	6.70706	13.4141	7.02006
2.886	2.598	0.288	600	0.628	4.56	0.912	6.57018	13.1404	6.87679
2.886	2.484	0.402	900	0.942	4.45	0.89	6.11392	12.2278	6.39924
2.886	2.387	0.499	1200	1.256	4.325	0.865	5.69188	11.3838	5.95750
2.886	2.332	0.554	1500	1.571	3.471	0.6942	5.05539	10.1108	5.29131

Table 4.13

Weight Fraction- 10% Load- 5 N Velocities – 1.571 m/s

m_1 (gm)	m_2 (gm)	Δm (gm)	t (sec)	$SD\times10^3$ (m)	F_f (N)	μ	$W_r \times10^{-10}$ (m^3/m)	$W_s \times10^{-11}$ (m^3/Nm)	$W_v \times10^{-10}$ (m^3/s)
1.894	1.615	0.279	300	0.471	4.6	0.92	8.48649	16.9730	13.3238
1.894	1.402	0.492	600	0.942	4.56	0.912	7.48271	14.9654	11.7479
1.894	1.352	0.542	900	1.413	4.45	0.89	5.49543	10.9909	8.62783
1.894	1.238	0.656	1200	1.884	4.325	0.865	4.98847	9.97694	7.83190
1.894	1.167	0.727	1500	2.355	3.471	0.6942	4.42271	8.84541	6.94365

Table 4.14

Weight Fraction- 10% Load- 5 N Velocity – 2.094 m/s

m_1 (gm)	m_2 (gm)	Δm (gm)	t (sec)	$SD\times10^3$ (m)	F_f (N)	μ	$W_r \times10^{-10}$ (m^3/m)	$W_s \times10^{-11}$ (m^3/Nm)	$W_v \times10^{-10}$ (m^3/s)
2.465	2.037	0.428	300	0.628	4.6	0.92	9.75961	19.5280	20.4394
2.465	1.779	0.686	600	1.256	4.56	0.912	7.83337	15.6498	16.3801
2.465	1.544	0.921	900	1.884	4.45	0.89	7.00937	14.0073	14.6609
2.465	1.434	1.031	1200	2.512	4.325	0.865	5.88305	11.7602	12.3090
2.465	1.393	1.072	1500	3.141	3.471	0.6942	4.89264	9.78227	10.2388

Table 4.15

Weight Fraction- 10% Load- 10 N Velocity – 1.047 m/s

m_1 (gm)	m_2 (gm)	Δm (gm)	t (sec)	$SD\times10^3$ (m)	F_f (N)	μ	$W_r \times10^{-10}$ (m^3/m)	$W_s \times10^{-11}$ (m^3/Nm)	$W_v \times10^{-10}$ (m^3/s)
2.604	2.375	0.229	300	0.314	5.7	0.57	10.5849	10.58490	10.9360
2.604	2.304	0.3	600	0.628	5.47	0.547	6.93334	6.93334	7.16332
2.604	2.253	0.351	900	0.942	4.9	0.49	5.40800	5.40800	5.58739
2.604	2.207	0.397	1200	1.256	4.34	0.434	4.58756	4.58756	4.73973
2.604	2.177	0.427	1500	1.571	4.015	0.4015	3.94738	3.94738	4.07832

Table 4.16

Weight Fraction- 10% Load- 10 N Velocity – 1.571 m/s

m_1 (gm)	m_2 (gm)	Δm (gm)	t (sec)	$SD\times10^3$ (m)	F_f (N)	μ	$W_r \times10^{-10}$ (m^3/m)	$W_s \times10^{-11}$ (m^3/Nm)	$W_v \times10^{-10}$ (m^3/s)
2.104	1.72	0.384	300	0.471	4.733	0.4733	11.6803	11.6803	18.3381
2.104	1.525	0.579	600	0.942	3.557	0.3557	8.80587	8.80587	13.8252
2.104	1.469	0.635	900	1.413	3.501	0.3501	6.43837	6.43837	10.1082
2.104	1.431	0.673	1200	1.884	3.4	0.34	5.11775	5.11775	8.03486
2.104	1.319	0.785	1500	2.355	3.0	0.3	4.77555	4.77555	7.49761

Table 4.17

Weight Fraction- 10% Load- 10N Velocity – 2.094 m/s

m_1 (gm)	m_2 (gm)	Δm (gm)	t (sec)	$SD\times10^3$ (m)	F_f (N)	μ	$W_r \times10^{-10}$ (m^3/m)	$W_s \times10^{-11}$ (m^3/Nm)	$W_v \times10^{-10}$ (m^3/s)
2.974	2.538	0.436	300	0.628	5.0	0.50	9.94653	9.94653	20.8214
2.974	2.276	0.698	600	1.256	4.7	0.47	7.96178	7.96178	16.6667
2.974	2.051	0.923	900	1.884	3.44	0.344	7.01884	7.01884	14.6928
2.974	1.905	1.069	1200	2.512	2.62	0.262	6.09681	6.09681	12.7627
2.974	1.738	1.236	1500	3.141	2.41	0.241	5.63941	5.63941	11.8052

Table 4.18

Weight Fraction-10% Load- 15 N Velocity – 1.047 m/s

m_1 (gm)	m_2 (gm)	Δm (gm)	t (sec)	$SD\times10^3$ (m)	F_f (N)	μ	$W_r \times10^{-10}$ (m^3/m)	$W_s \times10^{-11}$ (m^3/Nm)	$W_v \times10^{-10}$ (m^3/s)
2.924	2.729	0.195	300	0.314	7.65	0.510	8.89712	5.93141	9.31232
2.924	2.632	0.292	600	0.628	7.38	0.492	6.66143	4.44096	6.97230
2.924	2.541	0.383	900	0.942	7.05	0.470	5.82495	3.8833	6.09678
2.924	2.462	0.462	1200	1.256	6.95	0.463	5.26983	3.51322	5.51576
2.924	2.402	0.522	1500	1.571	6.82	0.454	4.76338	3.17559	4.98567

Table 4.19

Weight Fraction- 10% Load- 15 N Velocity – 1.571 m/s

m_1 (gm)	m_2 (gm)	Δm (gm)	t (sec)	$SD\times10^3$ (m)	F_f (N)	μ	$W_r \times10^{-10}$ (m^3/m)	$W_s \times10^{-11}$ (m^3/Nm)	$W_v \times10^{-10}$ (m^3/s)
2.424	2.001	0.423	300	0.471	7.65	0.510	12.8666	8.57774	20.2006
2.424	1.827	0.597	600	0.942	7.05	0.470	9.07963	6.05308	14.2550
2.424	1.762	0.662	900	1.413	7.00	0.466	6.71213	4.47475	10.5380
2.424	1.735	0.689	1200	1.884	5.98	0.398	5.23942	3.49294	8.22588
2.424	1.708	0.716	1500	2.355	5.32	0.354	4.35579	2.90386	6.83859

Table 4.20

Weight Fraction- 10% Load- 15 N Velocity – 2.094 m/s

m_1 (gm)	m_2 (gm)	Δm (gm)	t (sec)	$SD\times10^3$ (m)	F_f (N)	μ	$W_r \times10^{-10}$ (m^3/m)	$W_s \times10^{-11}$ (m^3/Nm)	$W_v \times10^{-10}$ (m^3/s)
2.619	2.109	0.510	300	0.628	6.23	0.415	11.6216	7.75647	24.3553
2.619	1.804	0.815	600	1.256	5.90	0.393	9.29410	6.19757	19.4604
2.619	1.540	1.079	900	1.884	5.76	0.384	8.20791	5.47008	17.1761
2.619	1.322	1.297	1200	2.512	5.36	0.357	7.39996	4.93144	15.4847
2.619	1.139	1.480	1500	3.141	5.20	0.346	6.75467	4.50179	14.1356

Table 4.21

Weight Fraction- 15% Load- 5 N Velocity – 1.047 m/s

m_1 (gm)	m_2 (gm)	Δm (gm)	t (sec)	$SD\times10^3$ (m)	F_f (N)	μ	$W_r \times10^{-10}$ (m^3/m)	$W_s \times10^{-11}$ (m^3/Nm)	$W_v \times10^{-10}$ (m^3/s)
2.989	2.889	0.100	300	0.314	4.38	0.876	5.50037	11.0007	5.75705
2.989	2.819	0.170	600	0.628	4.26	0.852	4.67531	9.35063	4.89349
2.989	2.762	0.227	900	0.942	4.22	0.844	4.16195	8.32389	4.35617
2.989	2.703	0.286	1200	1.256	4.16	0.832	3.93276	7.86553	4.11629
2.989	2.65	0.339	1500	1.571	3.471	0.6942	3.72925	7.4585	3.90328

Table 4.22

Weight Fraction- 15% Load- 5 N Velocity – 1.571 m/s

m_1 (gm)	m_2 (gm)	Δm (gm)	t (sec)	$SD\times10^3$ (m)	F_f (N)	μ	$W_r \times10^{-10}$ (m^3/m)	$W_s \times10^{-11}$ (m^3/Nm)	$W_v \times10^{-10}$ (m^3/s)
2.659	2.502	0.157	300	0.471	4.42	0.884	5.75705	11.5141	9.03857
2.659	2.378	0.281	600	0.942	4.11	0.822	5.15201	10.3040	8.08866
2.659	2.287	0.372	900	1.413	3.86	0.772	4.54697	9.09394	7.13874
2.659	2.250	0.409	1200	1.884	3.71	0.742	3.74942	7.49884	5.88659
2.659	2.233	0.426	1500	2.355	3.69	0.738	3.12421	6.24842	4.90501

Table 4.23

Weight Fraction- 15% Load- 5 N Velocity – 2.094 m/s

m_1 (gm)	m_2 (gm)	Δm (gm)	t (sec)	$SD\times10^3$ (m)	F_f (N)	μ	$W_r \times10^{-10}$ (m^3/m)	$W_s \times10^{-11}$ (m^3/Nm)	$W_v \times10^{-10}$ (m^3/s)
2.301	2.044	0.257	300	0.628	4.77	0.954	7.06797	14.1359	14.7956
2.301	1.882	0.419	600	1.256	4.40	0.880	5.76164	11.5233	12.0610
2.301	1.780	0.521	900	1.884	4.22	0.844	4.77615	9.55231	9.99808
2.301	1.689	0.612	1200	2.512	4.15	0.830	4.20778	8.41556	8.80829
2.301	1.610	0.691	1500	3.141	4.06	0.812	3.80075	7.60151	7.95625

Table 4.24

Weight Fraction-15% Load- 10 N Velocity – 1.047 m/s

m_1 (gm)	m_2 (gm)	Δm (gm)	t (sec)	$SD\times10^3$ (m)	F_f (N)	μ	$W_r \times10^{-10}$ (m^3/m)	$W_s \times10^{-11}$ (m^3/Nm)	$W_v \times10^{-10}$ (m^3/s)
2.881	2.706	0.175	300	0.314	9.22	0.922	9.62564	9.62564	10.0748
2.881	2.645	0.236	600	0.628	8.98	0.898	6.49043	6.49043	6.79332
2.881	2.606	0.275	900	0.942	8.70	0.870	5.042	5.04200	5.27730
2.881	2.565	0.316	1200	1.256	8.34	0.834	4.34529	4.34529	4.54807
2.881	2.515	0.366	1500	1.571	8.02	0.802	4.02627	4.02627	4.21416

Table 4.25

Weight Fraction- 15% Load- 10 N Velocity – 1.571 m/s

m_1 (gm)	m_2 (gm)	Δm (gm)	t (sec)	$SD\times10^3$ (m)	F_f (N)	μ	$W_r \times10^{-10}$ (m^3/m)	$W_s \times10^{-11}$ (m^3/Nm)	$W_v \times10^{-10}$ (m^3/s)
3.009	2.723	0.286	300	0.471	8.66	0.866	10.4874	10.4874	16.4652
3.009	2.652	0.357	600	0.942	7.80	0.780	6.54544	6.54544	10.2763
3.009	2.584	0.425	900	1.413	7.16	0.716	5.19479	5.19479	8.15582
3.009	2.504	0.505	1200	1.884	6.86	0.686	4.62948	4.62948	7.26828
3.009	2.474	0.535	1500	2.355	6.79	0.679	3.9236	3.9236	6.16005

Table 4.26

Weight Fraction- 15% Load- 10 N Velocity – 2.094 m/s

m_1 (gm)	m_2 (gm)	Δm (gm)	t (sec)	$SD\times10^3$ (m)	F_f (N)	μ	$W_r \times10^{-10}$ (m^3/m)	$W_s \times10^{-11}$ (m^3/Nm)	$W_v \times10^{-10}$ (m^3/s)
2.663	2.251	0.412	300	0.628	8.96	0.896	11.3308	11.3308	23.7191
2.663	2.097	0.566	600	1.256	7.81	0.781	7.78302	7.78302	16.2925
2.663	2.024	0.639	900	1.884	7.21	0.721	5.85789	5.85789	12.2625
2.663	1.976	0.687	1200	2.512	6.96	0.696	4.72344	4.72344	9.88774
2.663	1.952	0.711	1500	3.141	6.79	0.679	3.91076	3.91076	8.18653

Table 4.27

Weight Fraction- 15% Load- 15 N Velocity – 1.047m/s

m_1 (gm)	m_2 (gm)	Δm (gm)	t (sec)	$SD\times10^3$ (m)	F_f (N)	μ	$W_r \times10^{-10}$ (m^3/m)	$W_s \times10^{-11}$ (m^3/Nm)	$W_v \times10^{-10}$ (m^3/s)
2.351	2.165	0.186	300	0.314	12.05	0.803	10.2307	6.82046	10.7081
2.351	2.115	0.236	600	0.628	10.07	0.671	6.49043	4.32696	6.79332
2.351	2.083	0.268	900	0.942	9.82	0.654	4.91366	3.27578	5.14297
2.351	2.037	0.314	1200	1.256	9.60	0.640	4.31779	2.87853	4.51929
2.351	2.001	0.35	1500	1.571	9.52	0.634	3.84781	2.5652	4.02994

Table 4.28

Weight Fraction- 15% Load- 15 N Velocity – 1.571 m/s

m_1 (gm)	m_2 (gm)	Δm (gm)	t (sec)	$SD\times10^3$ (m)	F_f (N)	μ	$W_r \times10^{-10}$ (m^3/m)	$W_s \times10^{-11}$ (m^3/Nm)	$W_v \times10^{-10}$ (m^3/s)
2.847	2.529	0.318	300	0.471	12.95	0.863	11.6608	7.77385	18.3074
2.847	2.472	0.375	600	0.942	12.25	0.816	6.87546	4.58364	10.7945
2.847	2.461	0.386	900	1.413	11.67	0.778	4.71809	3.1454	7.40741
2.847	2.356	0.491	1200	1.884	10.95	0.730	4.50113	3.00076	7.06678
2.847	2.326	0.521	1500	2.355	10.51	0.700	3.82092	2.54728	5.99885

Table 4.29

Weight Fraction- 15% Load- 15 N Velocity – 2.094 m/s

m_1 (gm)	m_2 (gm)	Δm (gm)	t (sec)	$SD\times10^3$ (m)	F_f (N)	μ	$W_r \times10^{-10}$ (m^3/m)	$W_s \times10^{-11}$ (m^3/Nm)	$W_v \times10^{-10}$ (m^3/s)
2.255	1.827	0.428	300	0.628	13.71	0.914	11.7708	7.84719	24.6402
2.255	1.703	0.552	600	1.256	12.16	0.810	7.59051	5.06034	15.8895
2.255	1.636	0.619	900	1.884	11.88	0.792	5.67455	3.78303	11.8787
2.255	1.594	0.661	1200	2.512	11.07	0.738	4.54468	3.02979	9.51353
2.255	1.497	0.758	1500	3.141	10.55	0.703	4.16928	2.77952	8.72769

Table 4.30

Weight Fraction- 20% Load- 5 N Velocity – 1.047 m/s

m_1 (gm)	m_2 (gm)	Δm (gm)	t (sec)	$SD\times10^3$ (m)	F_f (N)	μ	$W_r \times10^{-10}$ (m^3/m)	$W_s \times10^{-11}$ (m^3/Nm)	$W_v \times10^{-10}$ (m^3/s)
2.746	2.646	0.100	300	0.314	4.67	0.934	6.42079	12.8416	6.72043
2.746	2.598	0.148	600	0.628	4.44	0.888	4.75139	9.50277	4.97312
2.746	2.559	0.187	900	0.942	4.05	0.810	4.00229	8.00459	4.18907
2.746	2.531	0.215	1200	1.256	4.00	0.800	3.45118	6.90235	3.61223
2.746	2.528	0.218	1500	1.571	3.94	0.788	2.79947	5.59893	2.93011

Table 4.31

Weight Fraction- 20% Load- 5 N Velocity – 1.571 m/s

m_1 (gm)	m_2 (gm)	Δm (gm)	t (sec)	$SD\times10^3$ (m)	F_f (N)	μ	$W_r \times10^{-10}$ (m^3/m)	$W_s \times10^{-11}$ (m^3/Nm)	$W_v \times10^{-10}$ (m^3/s)
2.823	2.676	0.147	300	0.471	4.70	0.940	6.29238	12.5848	9.87903
2.823	2.601	0.222	600	0.942	4.48	0.896	4.75139	9.50277	7.45968
2.823	2.55	0.273	900	1.413	4.06	0.812	3.89528	7.79056	6.11559
2.823	2.486	0.337	1200	1.884	3.81	0.762	3.60635	7.21269	5.66196
2.823	2.465	0.358	1500	2.355	3.41	0.682	3.06486	6.12972	4.81183

Table 4.32

Weight Fraction- 20% Load- 5 N Velocity – 2.094 m/s

m_1 (gm)	m_2 (gm)	Δm (gm)	t (sec)	$SD\times10^3$ (m)	F_f (N)	μ	$W_r \times10^{-10}$ (m^3/m)	$W_s \times10^{-11}$ (m^3/Nm)	$W_v \times10^{-10}$ (m^3/s)
3.085	2.857	0.228	300	0.628	4.36	0.872	7.3197	14.6394	15.3226
3.085	2.782	0.303	600	1.256	3.76	0.752	4.86375	9.7275	10.1815
3.085	2.727	0.358	900	1.884	3.51	0.702	3.83107	7.66215	8.01971
3.085	2.649	0.436	1200	2.512	3.45	0.69	3.49933	6.99866	7.32527
3.085	2.578	0.507	1500	3.141	3.38	0.676	3.25534	6.51068	6.81452

Table 4.33

Weight Fraction- 20% Load- 10 N Velocity – 1.047 m/s

m_1 (gm)	m_2 (gm)	Δm (gm)	t (sec)	$SD \times 10^3$ (m)	F_f (N)	μ	$W_r \times 10^{-10}$ (m^3/m)	$W_s \times 10^{-11}$ (m^3/Nm)	$W_v \times 10^{-10}$ (m^3/s)
2.051	1.951	0.100	300	0.314	7.02	0.702	6.42079	6.42079	6.72043
2.051	1.894	0.157	600	0.628	6.80	0.680	5.04032	5.04032	5.27554
2.051	1.866	0.185	900	0.942	6.52	0.652	3.95949	3.95949	4.14427
2.051	1.842	0.209	1200	1.256	6.32	0.632	3.35486	3.35486	3.51142
2.051	1.823	0.228	1500	1.571	6.26	0.626	2.92788	2.92788	3.06452

Table 4.33

Weight Fraction- 20% Load- 10 N Velocity – 1.571 m/s

m_1 (gm)	m_2 (gm)	Δm (gm)	t (sec)	$SD \times 10^3$ (m)	F_f (N)	μ	$W_r \times 10^{-10}$ (m^3/m)	$W_s \times 10^{-11}$ (m^3/Nm)	$W_v \times 10^{-10}$ (m^3/s)
2.721	2.563	0.158	300	0.471	7.32	0.732	6.76324	6.76324	10.6183
2.721	2.504	0.217	600	0.942	7.07	0.707	4.64437	4.64437	7.29167
2.721	2.443	0.278	900	1.413	6.44	0.644	3.96662	3.96662	6.22760
2.721	2.387	0.334	1200	1.884	5.86	0.586	3.57424	3.57424	5.61156
2.721	2.338	0.383	1500	2.355	5.65	0.565	3.27889	3.27889	5.14785

Table 4.34

Weight Fraction- 20% Load- 10 N Velocity – 2.094 m/s

m_1 (gm)	m_2 (gm)	Δm (gm)	t (sec)	$SD\times10^3$ (m)	F_f (N)	μ	$W_r \times10^{-10}$ (m^3/m)	$W_s \times10^{-11}$ (m^3/Nm)	$W_v \times10^{-10}$ (m^3/s)
2.568	2.321	0.247	300	0.628	7.80	0.780	7.92968	7.92968	16.5995
2.568	2.272	0.296	600	1.256	6.47	0.647	4.75139	4.75139	9.94624
2.568	2.171	0.397	900	1.884	5.60	0.560	4.24842	4.24842	8.89337
2.568	2.114	0.454	1200	2.512	4.77	0.477	3.6438	3.6438	7.62769
2.568	2.051	0.517	1500	3.141	4.23	0.423	3.31955	3.31955	6.94892

Table 4.35

Weight Fraction-20% Load- 15 N Velocity – 1.047 m/s

m_1 (gm)	m_2 (gm)	Δm (gm)	t (sec)	$SD\times10^3$ (m)	F_f (N)	μ	$W_r \times10^{-10}$ (m^3/m)	$W_s \times10^{-11}$ (m^3/Nm)	$W_v \times10^{-10}$ (m^3/s)
2.725	2.620	0.105	300	0.314	12.77	0.851	6.74183	4.49456	7.05645
2.725	2.556	0.169	600	0.628	11.81	0.787	5.42557	3.61705	5.67876
2.725	2.498	0.227	900	0.942	11.14	0.742	4.85840	3.23893	5.08513
2.725	2.470	0.255	1200	1.256	10.78	0.718	4.09326	2.72884	4.28427
2.725	2.438	0.287	1500	1.571	10.52	0.701	3.68319	2.45546	3.85753

Table 4.36

Weight Fraction- 20% Load- 15 N Velocity – 1.571m/s

m_1 (gm)	m_2 (gm)	Δm (gm)	t (sec)	$SD\times10^3$ (m)	F_f (N)	μ	$W_r \times10^{-10}$ (m^3/m)	$W_s \times10^{-11}$ (m^3/Nm)	$W_v \times10^{-10}$ (m^3/s)
2.726	2.511	0.215	300	0.471	12.15	0.810	9.20314	6.13542	14.44890
2.726	2.451	0.275	600	0.942	11.44	0.762	5.88573	3.92382	9.24059
2.726	2.42	0.306	900	1.413	11.05	0.736	4.36614	2.91076	6.85484
2.726	2.397	0.329	1200	1.884	10.52	0.701	3.52073	2.34716	5.52755
2.726	2.399	0.327	1500	2.355	10.14	0.676	2.79947	1.86631	4.39516

Table 4.37

Weight Fraction- 20% Load- 15 N Velocity – 2.094 m/s

m_1 (gm)	m_2 (gm)	Δm (gm)	t (sec)	$SD\times10^3$ (m)	F_f (N)	μ	$W_r \times10^{-10}$ (m^3/m)	$W_s \times10^{-11}$ (m^3/Nm)	$W_v \times10^{-10}$ (m^3/s)
1.929	1.577	0.352	300	0.628	11.40	0.760	11.3006	7.53373	23.6559
1.929	1.505	0.424	600	1.256	10.66	0.710	6.80604	4.53736	14.2473
1.929	1.436	0.493	900	1.884	9.95	0.663	5.27575	3.51717	11.0439
1.929	1.4	0.529	1200	2.512	9.575	0.638	4.24575	2.8305	8.88777
1.929	1.355	0.574	1500	3.141	9.475	0.631	3.68554	2.45702	7.71505

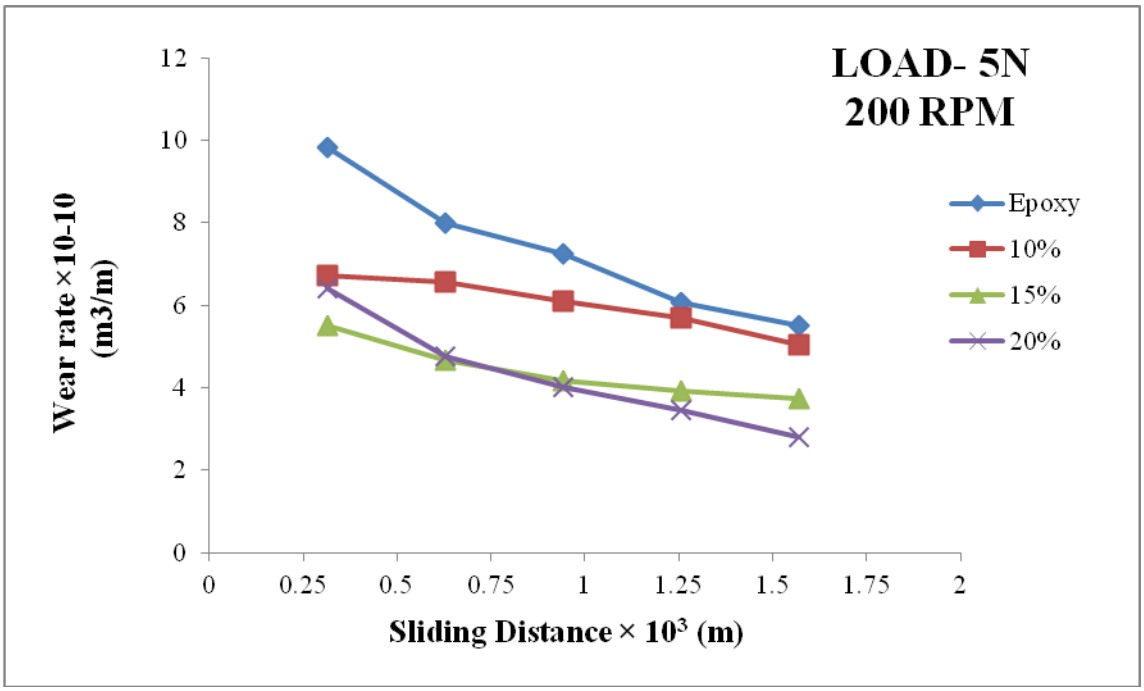

Fig.4.6: Variation of abrasive wear rate with sliding distance at 5N load and 200 rpm

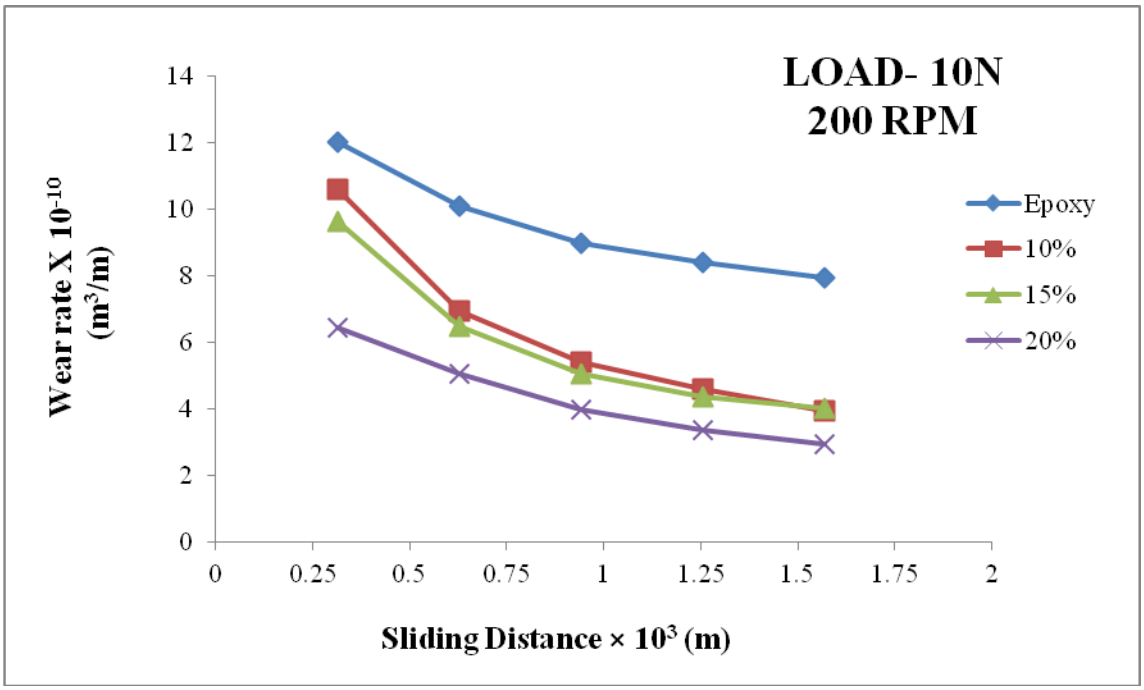

Fig.4.7: Variation of abrasive wear rate with sliding distance at 10 N load and 200 rpm

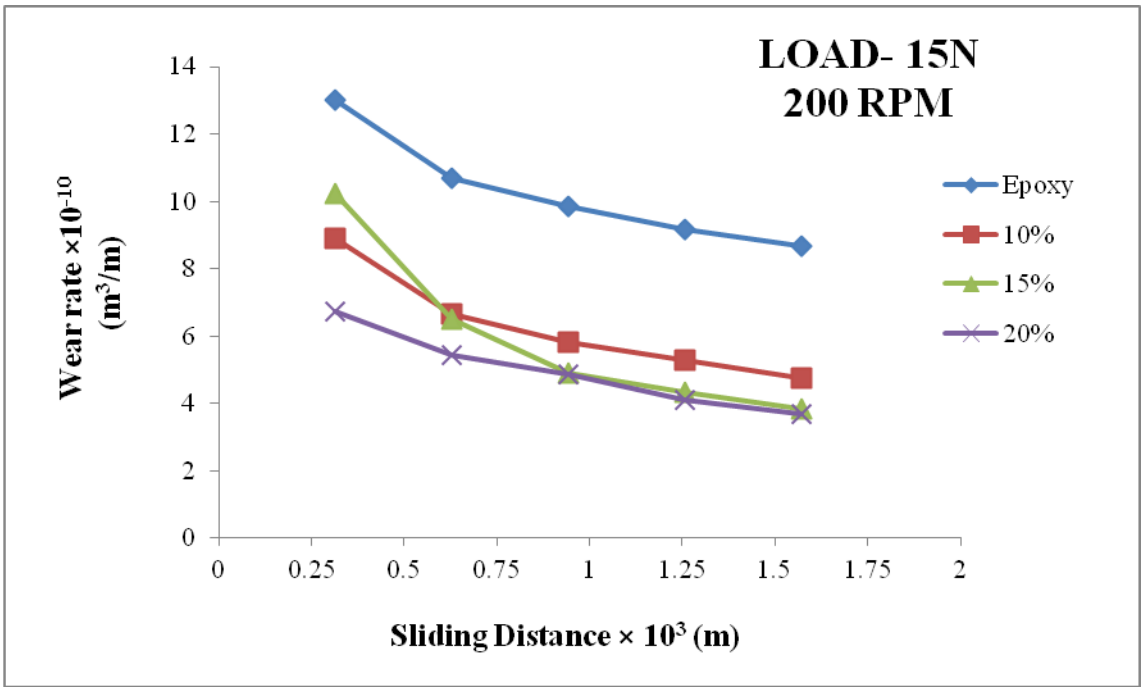

Fig.4.8: Variation of abrasive wear rate with sliding distance at 15 N load and 200 rpm

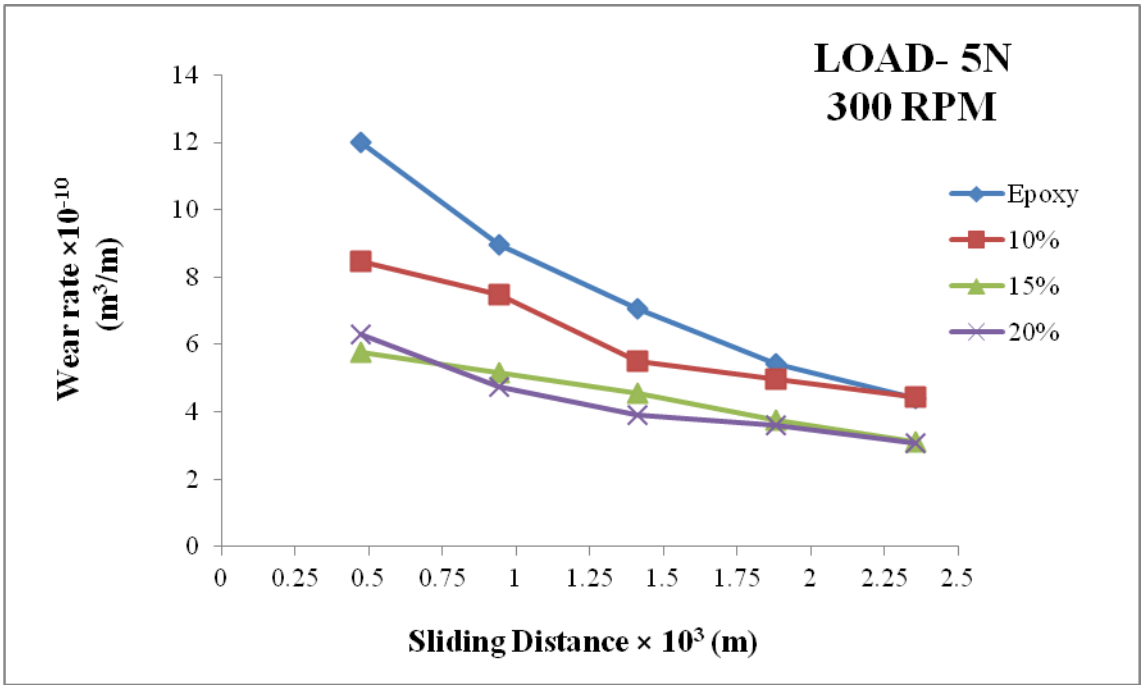

Fig.4.9: Variation of abrasive wear rate with sliding distance at 5 N load and 300 rpm

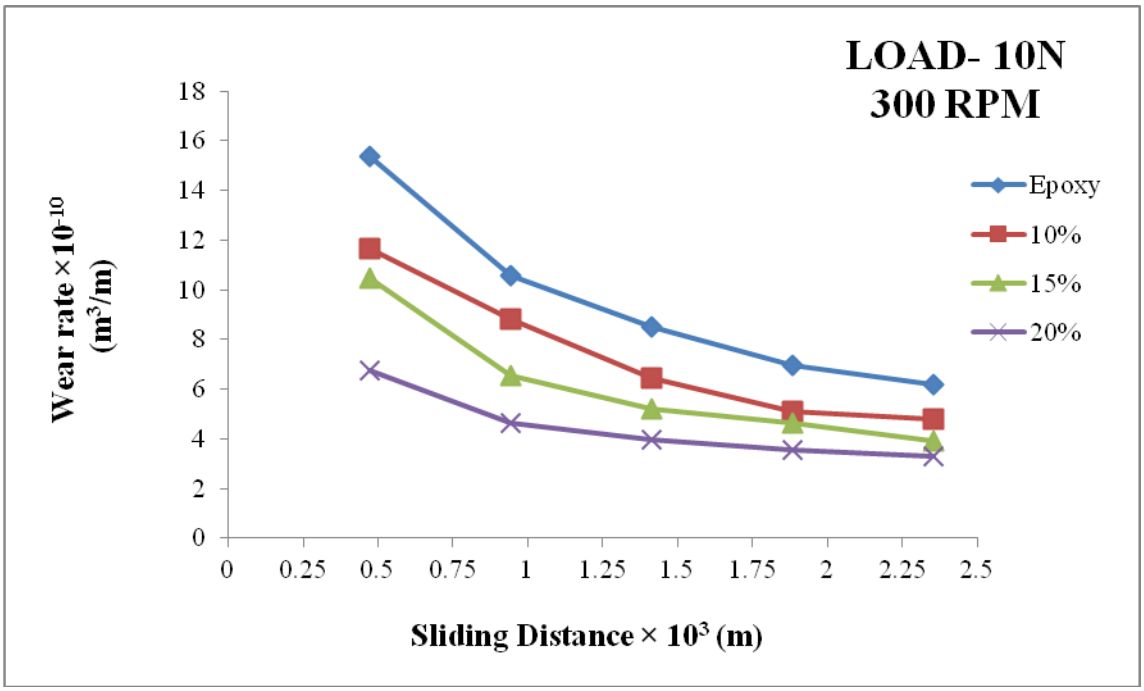

Fig.4.10: Variation of abrasive wear rate with sliding distance at 10 N load and 300 rpm

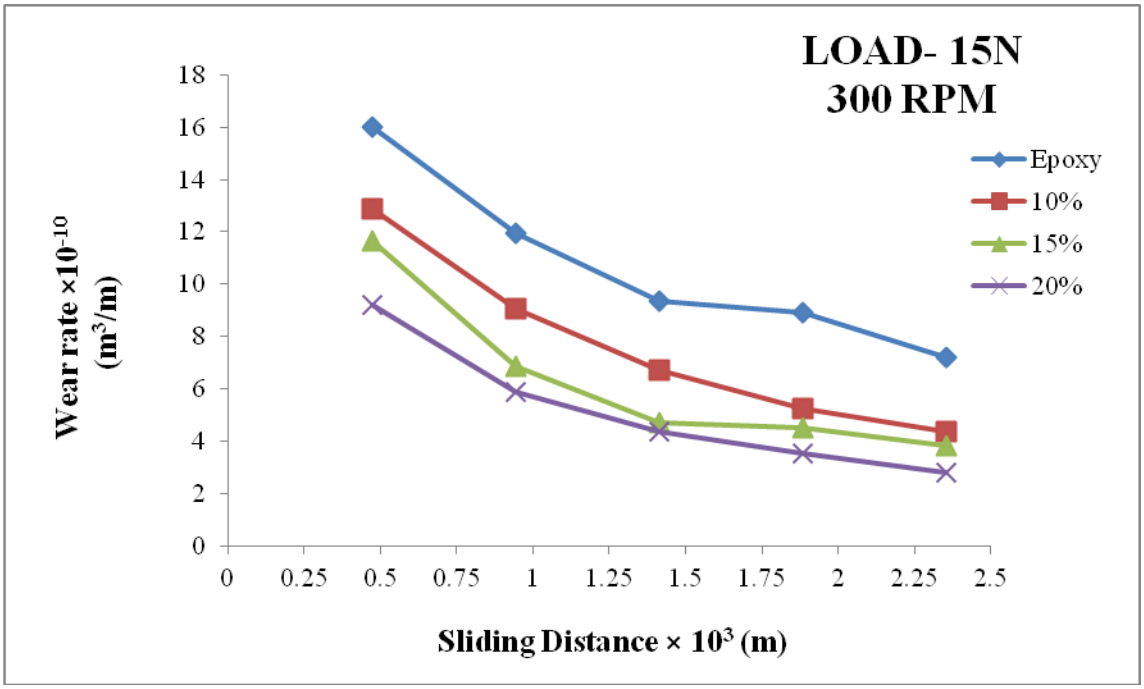

Fig.4.11: Variation of abrasive wear rate with sliding distance at 15 N load and 300 rpm

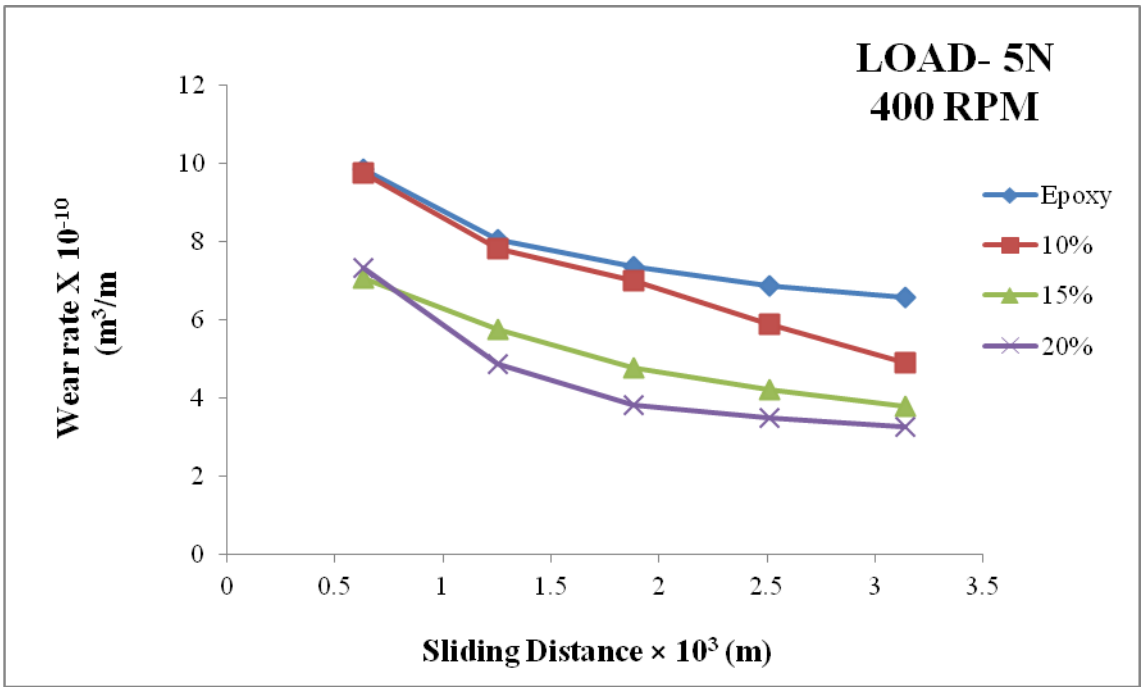

Fig.4.12: Variation of abrasive wear rate with sliding distance at 5 N load and 400 rpm

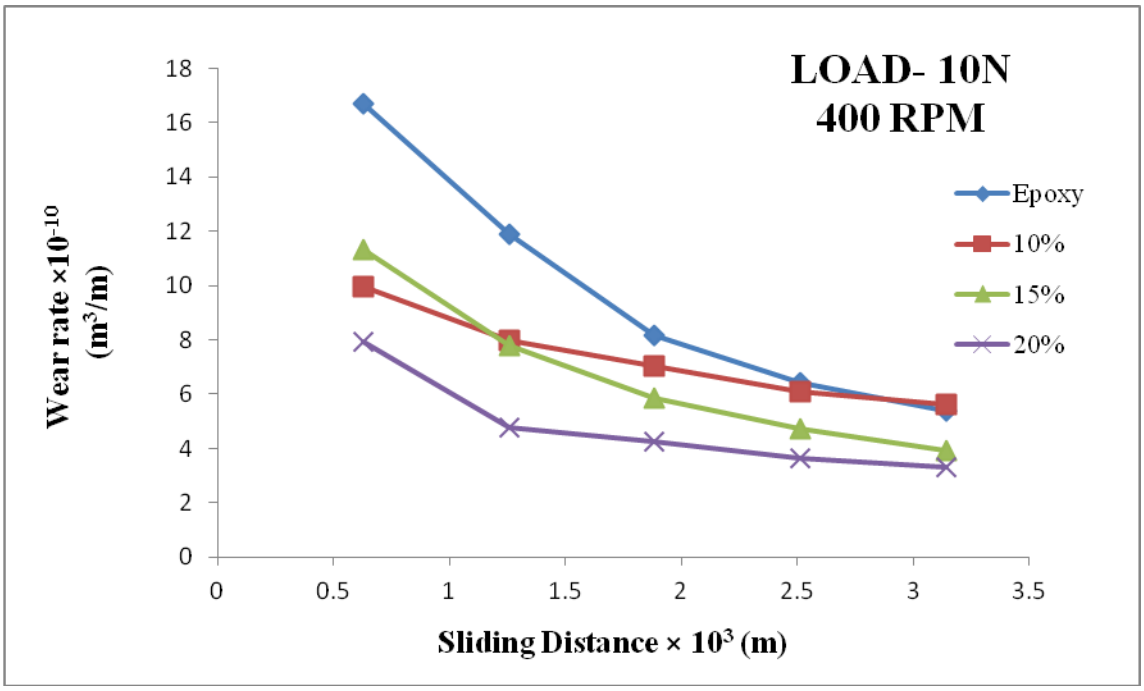

Fig.4.13: Variation of abrasive wear rate with sliding distance at 10 N load and 400 rpm

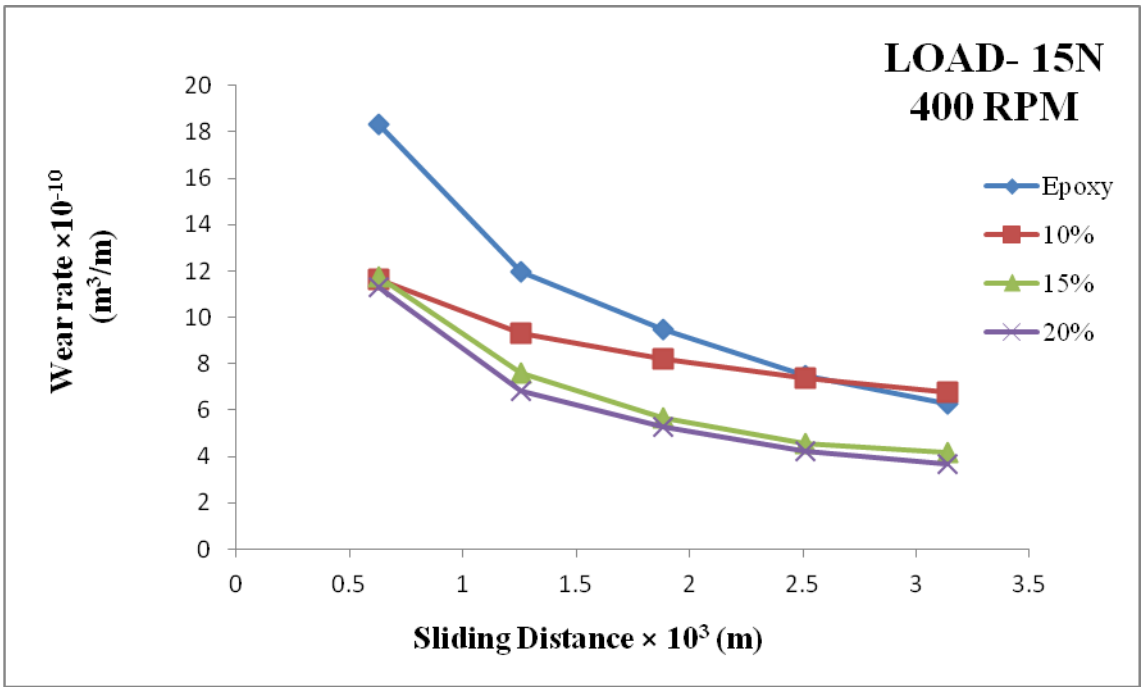

Fig.4.14: Variation of abrasive wear rate with sliding distance at 15 N load and 400 rpm

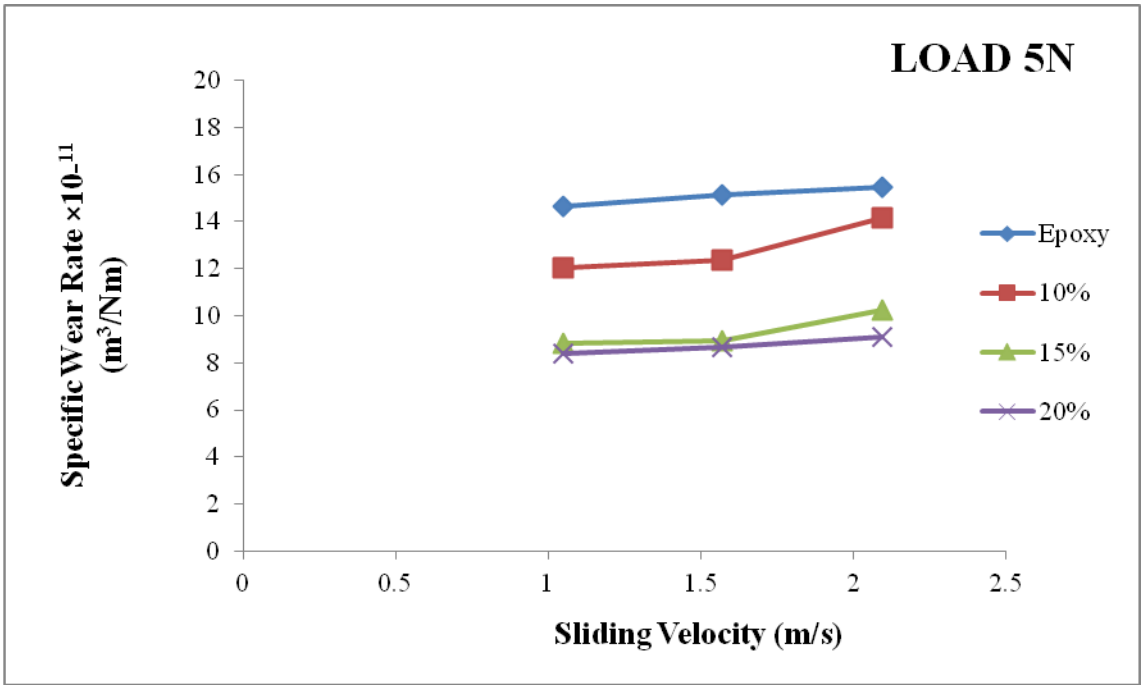

Fig.4.15: Variation of specific wear rate with sliding velocity at 5 N load

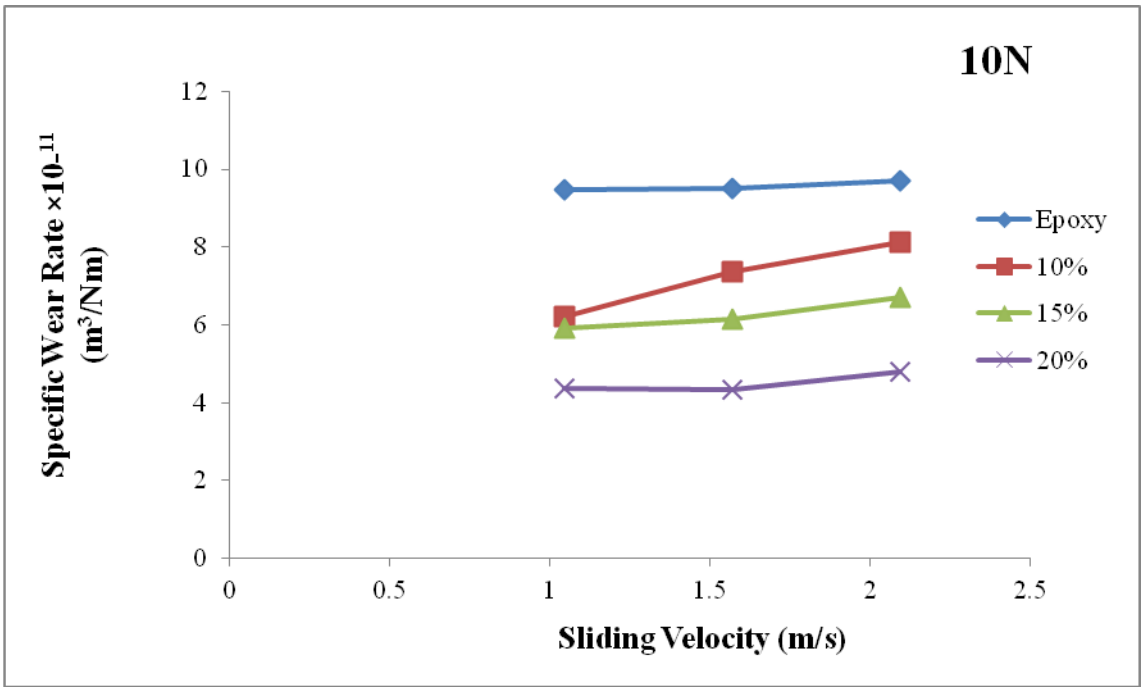

Fig.4.16: Variation of specific wear rate with sliding velocity at 10 N load

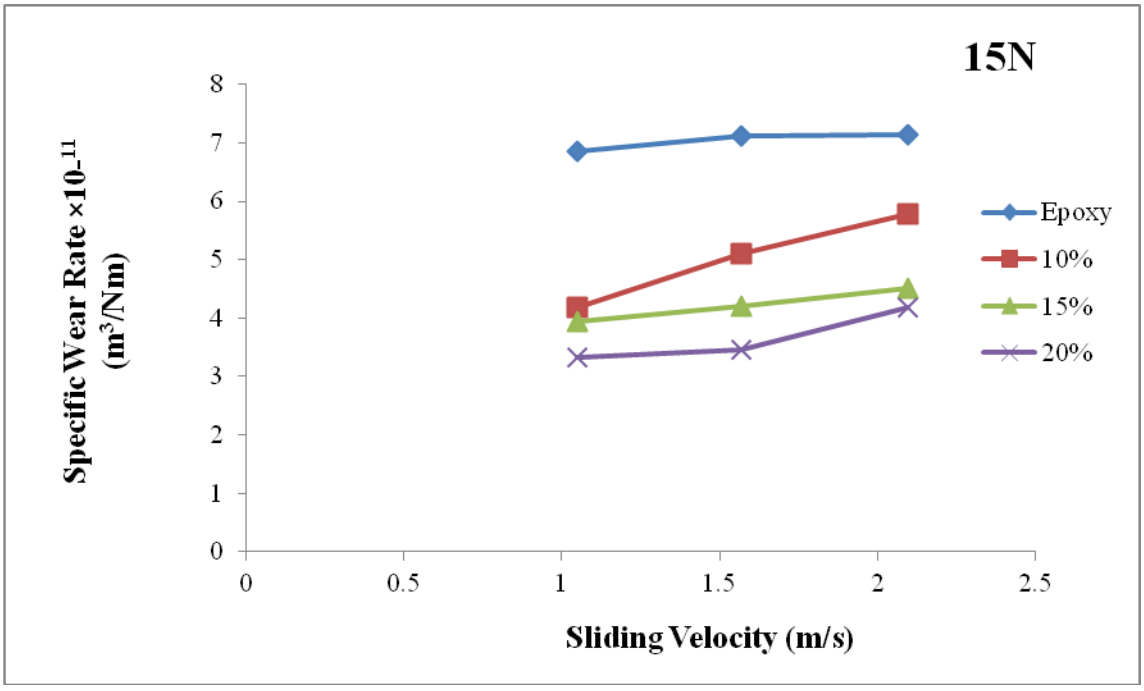

Fig.4.17: Variation of specific wear rate with sliding velocity at 15 N load

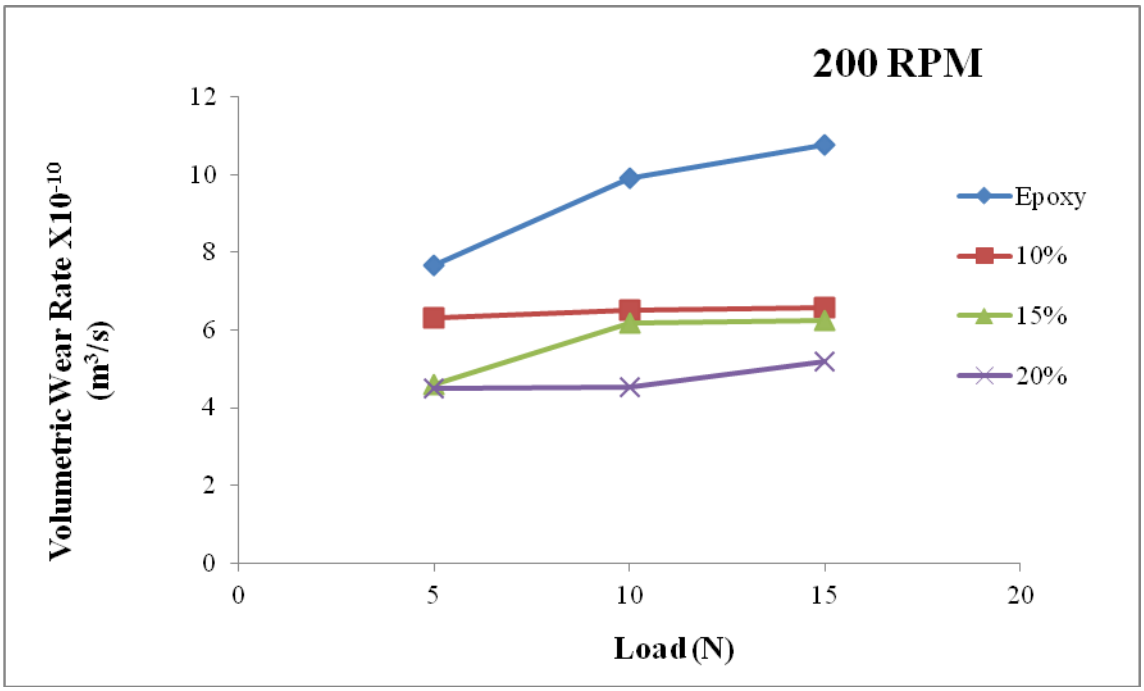

Fig.4.18: Variation of volumetric wear rate with load at 200 rpm

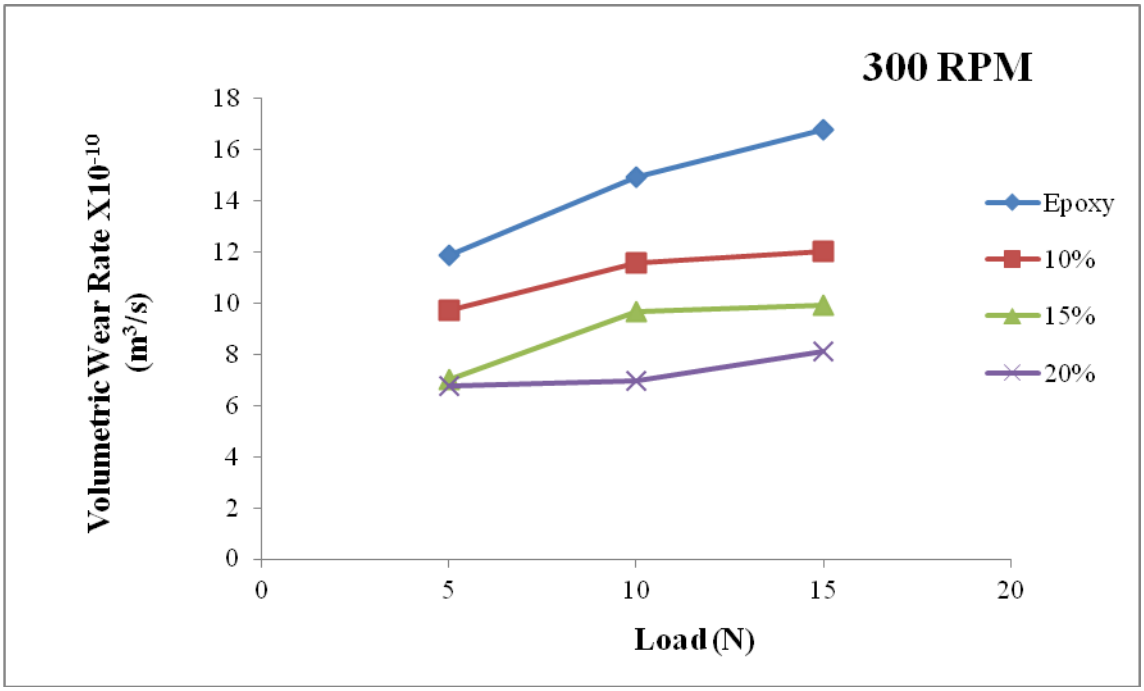

Fig.4.19: Variation of volumetric wear rate with load at 300 rpm

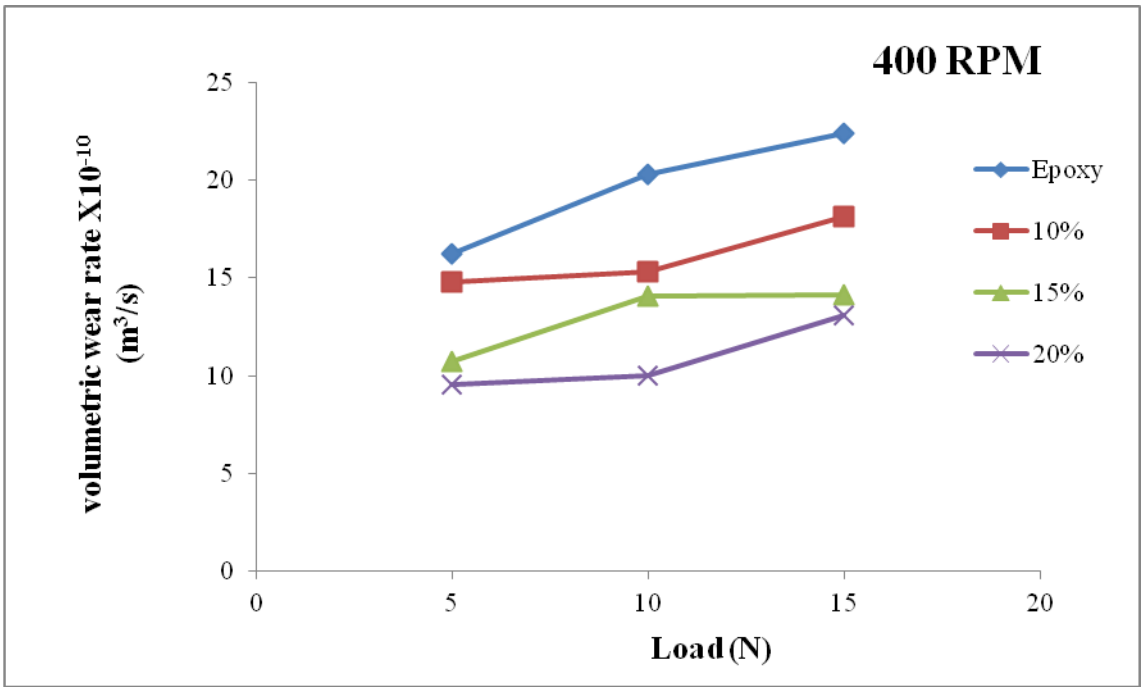

Fig.4.20: Variation of volumetric wear rate with load at 400 rpm

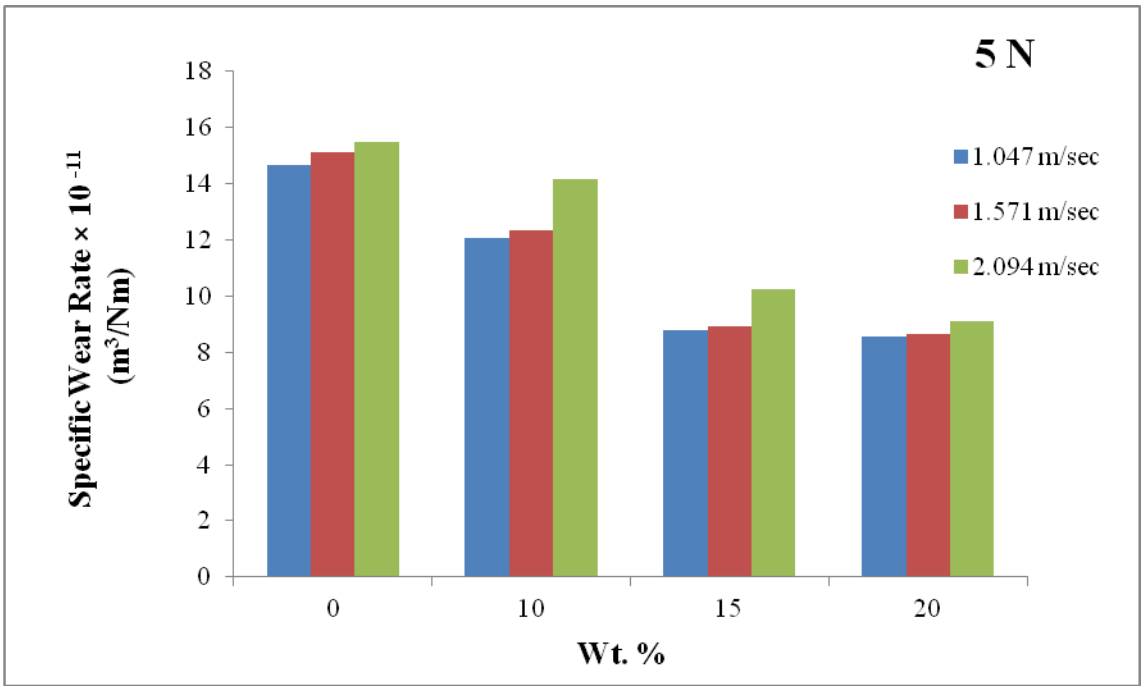

Fig.4.21: Variation of specific wear rate with Wt. % of filler at load 5 N

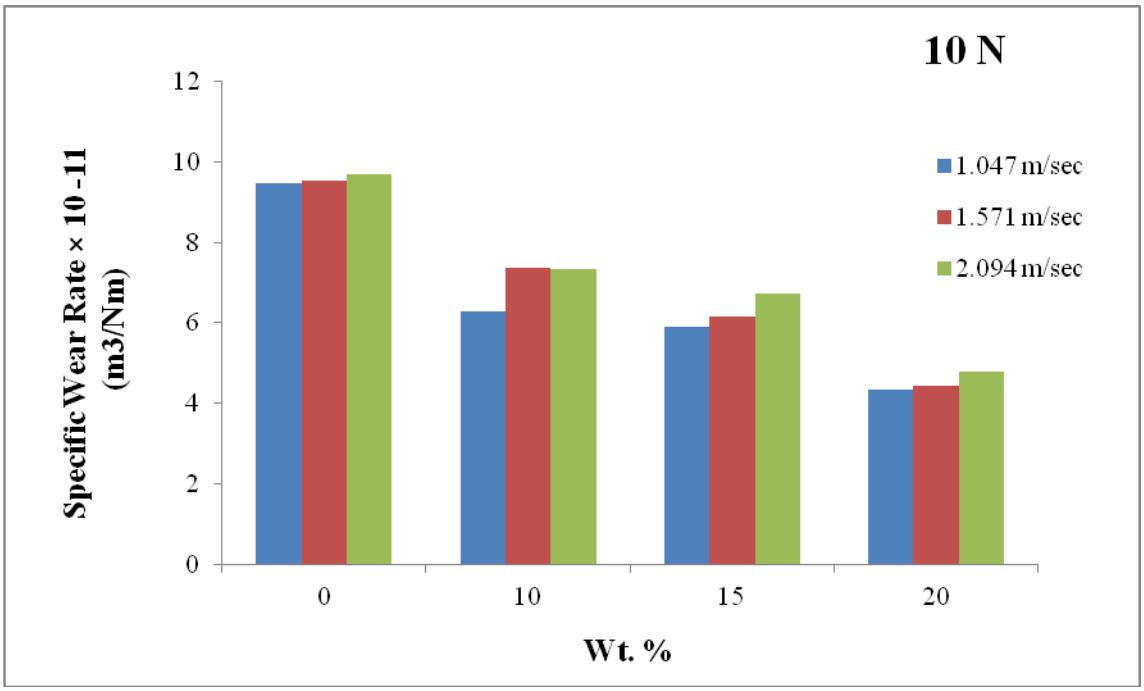

Fig.4.22: Variation of specific wear rate with Wt. % of filler at load 10 N

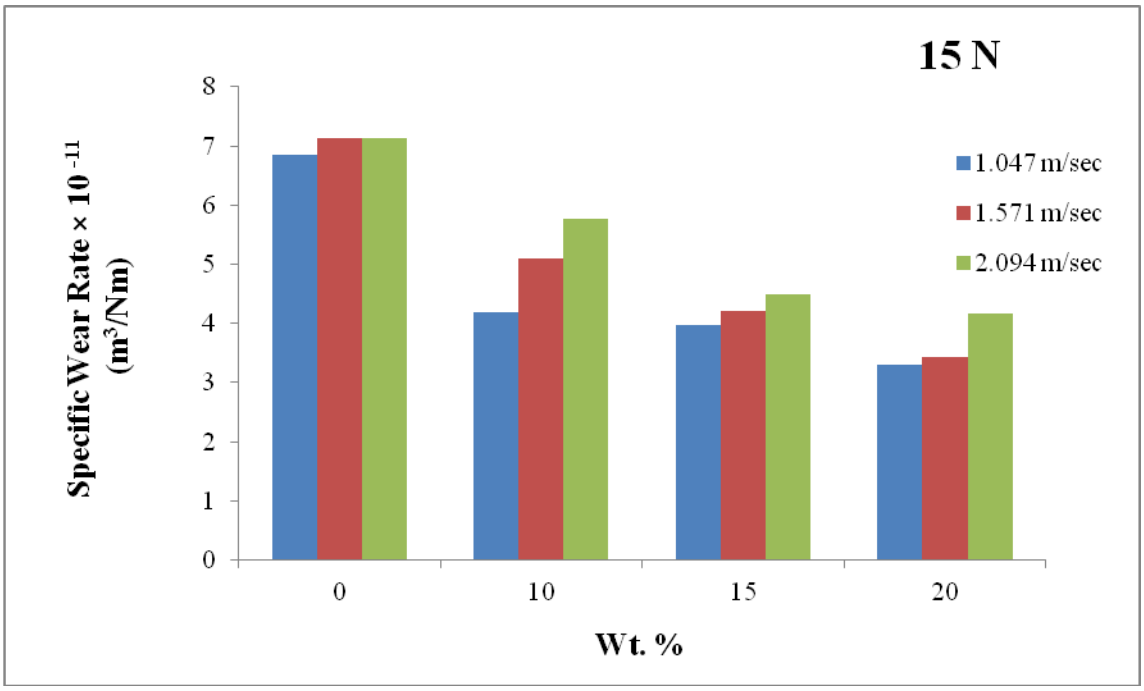

Fig.4.23: Variation of specific wear rate with Wt. % of filler at load 15 N

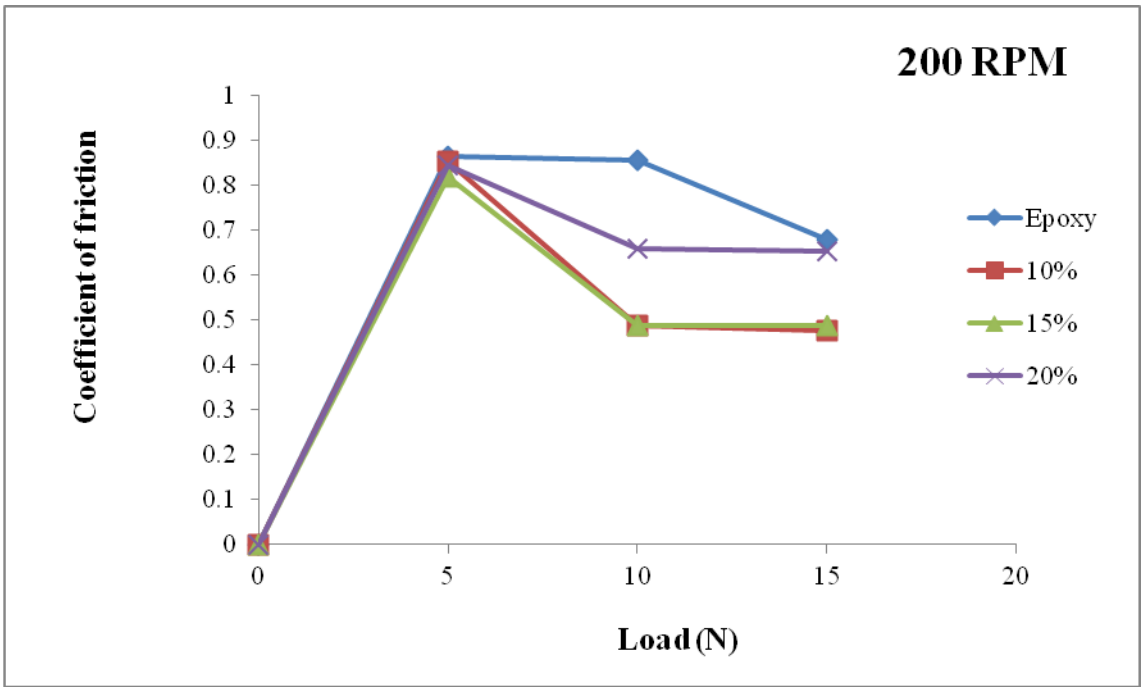

Fig.4.24: Variation of coefficient of friction with load at 200 rpm

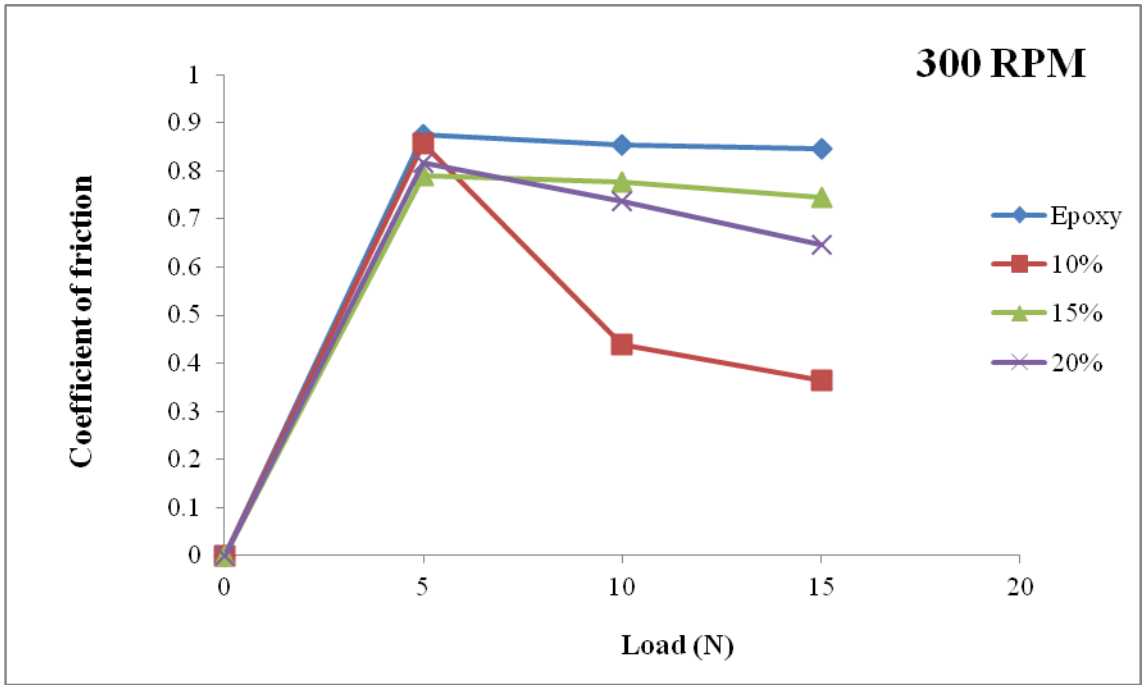

Fig.4.25: Variation of coefficient of friction with load at 300 rpm

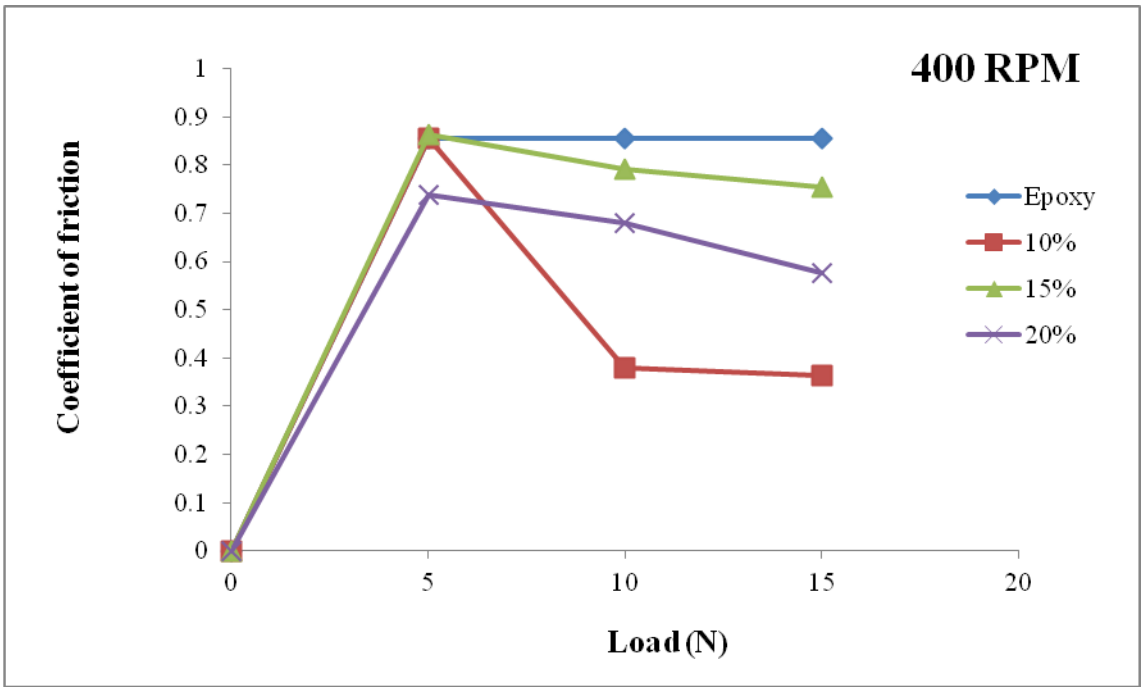

Fig.4.26: Variation of coefficient of friction with load at 400 rpm

4.3 SEM (Scanning Electron Microscope) Morphology :

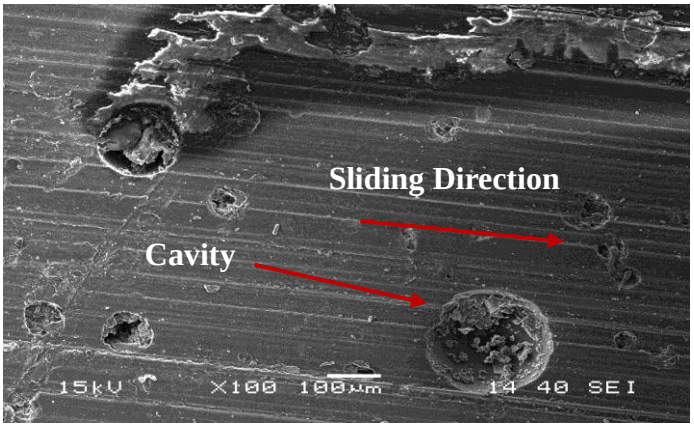

Fig.4.27: abrasive surface after test (10 % 10N 200 rpm)

It is clearly visible from the above micrograph that cavities are formed in the composite and aligned parallel to the direction of sliding. Some particles are also chipped off during sliding.

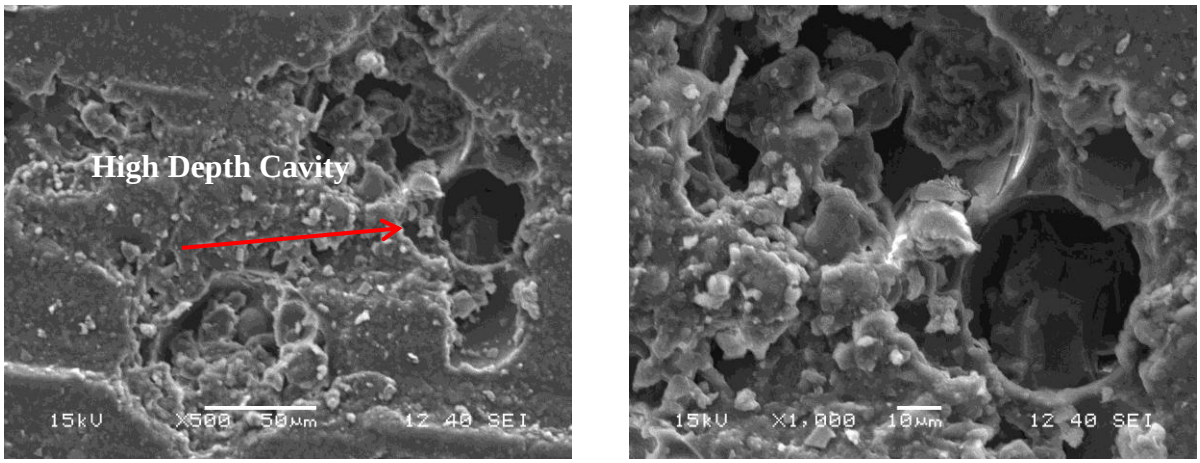

(a) (b)

Fig.4.28 (a) and (b): abrasive surface after test (20 % 10N 300 rpm)

In the above micrograpg cavities are formed with larger depth. Fig. 4.28(b) shows the depth of cavities at higher magnification. This might have happened due to the abrasive particles penetration and subsequent removal from the matrix at higher velocity.

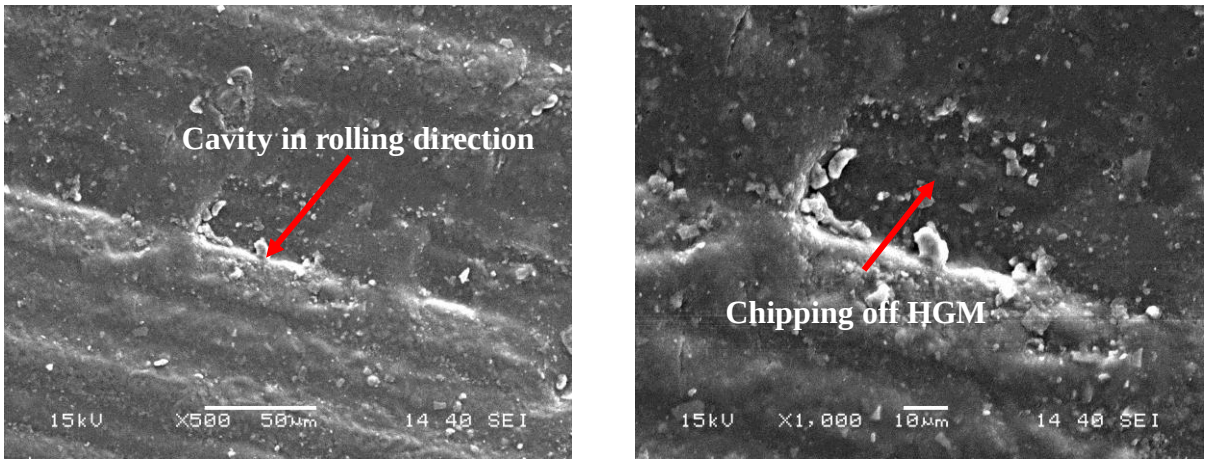

(a) (b)

Fig.4.29 (a) and (b): abrasive surface after test (20 % 10N 400 rpm)

In figure 4.29 (a) depth of cavities are less. Cavities are formed along the rolling direction. Chipping up of HGM particles are visible at some places but groove formation depth is less hence we get higher wear resistance. This might happened because at higher velocity (400 rpm) the abrasive particles are getting less time for penetration at a particular place. So that they did not formed deeper groove at removal particles from that location. Fig.4.29 (b) shows the same micrograph at higher magnification.

4.4 RESULTS AND DISCUSSION :

On the basis of experimental and tabulated (4.3 to 4.37) result several graphs are plotted and presented in fig. 4.6 to 4.26 for different weight fraction of hollow glass microsphere (HGM) as reinforcement under different test condition.

Figs. 4.6 to 4.14 exhibits the variation of dry sliding abrasive wear rate with increase in sliding distance for different rpm (200, 300 and 400) at different loads (5, 10 and 15 N). It is clear from the plots that with addition of hollow glass microsphere particulate the abrasive wear resistance of epoxy matrix increases. At longer sliding distance there is less exclusion of material because of low penetration of abrasive particles into the composite specimen. At 20 wt. % HGM abrasive wear rate is minimum at all testing conditions.

Fig. 4.15 to 4.17 shows the variation of specific wear rate of different wt. % (0, 10, 15 and 20) of filler composites with sliding velocity at different loads (5N, 10N and 15 N). From the plot it is clear that the specific wear rate increases as the sliding velocity increase from 1.0471 m/sec to 2.094 m/sec. This might happened due to generation of frictional heat at the interface.

S. Basavarajappa et al. [25] also examined the same behaviour of epoxy and glass composite filled with graphite and silicon carbide particulates.

The deviation of volumetric wear rate with normal applied loads for different wt. % of particulate filled composites at different sliding velocities is represented in figs. 4.18 to 4.20. Volumetric wear rate is increases with increase of normal applied loads. At low value of normal load i.e. 5 N the wear rate was comparatively low due to low diffusion and less number of abrasive particles in action with rubbing surfaces. At greater value of load large number of rough particles comes into action and produces large number of grooves due to which wear rate increases. C. Kanchanomai et al. [38] also observed the increase in volumetric wear loss with increase in normal applied load at all sliding speeds. Cirino et al. [39] examined the similar effect in case of carbon epoxy composite and Verma et al. [40] also examined the similar effect in case of GRP composite.

It is clear from the figs. 4.21 to 4.23 that with increase in wt. % (0, 10, 15 and 20) of HGM of filler the specific wear rate decrease and it is lowest for 20 wt. % filler.

Fig. 4.24 to 4.26 represents the variation of coefficient of friction with normal applied loads. It is clear from plot that at initial stage the value of friction coefficient is high but as the value of load is increase the value of friction coefficient decreases and finally it become steady. S.R. Chauhan et al. [41] also examined the same frictional behaviour for composite made by reinforcement of silicon carbide filled glass fibre and glass fibre in vinylester under water and dry lubricated sliding environment.

CHAPTER 5

CONCLUSION AND FUTURE SCOPE

Chapter 5

5.1 CONCLUSION

Following conclusion can be drawn from the experimental investigation:

1. Density of composite was low as compared to neat epoxy so it can be consider as an applicable light material. With increase in filler content the density of composite will decrease.

2. On increasing the filler content the impact and tensile strength of composite increases. Best mechanical properties were obtained at the filler content of 20 weight fraction.

3. The inclusion of hollow glass microsphere into epoxy can considerably increase abrasive wear resistance of composite. At filler content of 20 weight fraction better wear resistance properties were obtained.

4. On increasing sliding distance abrasive wear rate continuously decreases and reach upto a steady state in multi-pass situations.

5. Specific wear rate increase with increase in sliding velocity. Irrespective of load it is minimum for filler content of 20 weight fraction.

6. Coefficient of friction at initial stage it increases to a higher value but after some time it decreases and reached a steady state value.

5.2 SCOPE FOR FUTURE RESEARCH

1. The current research can be further extended to filler content beyond 20 weight fractions.

2. By surface modification bonding strength between filler and matrix can be increase so that better mechanical properties can be achieved.

3. Apart from hand lay-up and compression moulding technique other technique can be used for fabrication.

4. The current experimental work on composite has given better wear resistance for dry sliding wear test. This can further be extended to other tribological tests like erosion, dry sand abrasion test etc to make a final conclusion on the suitability of the developed composite for different applications.

REFERENCES:

References

[1]. Hutchings, I.M. (1992), Tribology: friction and wear of engineering materials. CRC Press.

[2]. Kranthi, G. & Satapathy, A. (2010), Evaluation and prediction of wear response of pine wood dust filled epoxy composites using neural computation. Computational Materials Science, 49, 609–614.

[3]. Gregory, S.W., Freudenberg, K.D., Bhimaraj, P. & Schadler, L.S. (2003), A study on the friction and wear behavior of PTFE filled with alumina nanoparticles. Wear, 254 (5-6), 573–580.

[4]. Rothon, R.N. (1999), Mineral fillers in thermoplastics: filler characterization and manufacture Advances in Polymer Science, 139, pp 67–107.

[5]. Suresha, B., Rajesh, B.N., Subbaya, K.M., Ravi Kumar, B.N. & Chandramohan, G. (2010), Influence of graphite filler on two-body abrasive wear behavior of carbon fabric reinforced epoxy composites. Materials and Design, 31, pp 1833–1841.

[6]. Mohan, N., Natarajan, S. & KumareshBabu, S.P. (2011), Abrasive wear behaviour of hard powders filled glass fabric epoxy hybrid composites. Materials and Design, 32, pp 1704–1709.

[7]. Schwartz, C.J. & Bahadur, S. (2001), The role of filler deformability, filler–polymer bending, and counterface material on the tribological behaviour of polyphenylene sulfide.Wear, 251, pp 1532–1540.

[8]. Nayak, R., Dora, P.T. & Satapathy, A. (2010), A computational and experimental investigation on thermal conductivity of particle reinforced epoxy composites. Computational Materials Science, 48, pp 576-581.

[9]. Callister, William D. Jr. Materials Science and Engineering: An Introduction, 7th edition. New York: John Wiley & Sons, Inc., 2007, pp 577 – 607. Print.

[10]. Peter J, Blau, "Fifty years of research on the wear of metals", Tribology International, 2007, Vol. 30, No. 5, pp 321-331.

[11]. M.F.Ashby and S.C.Lim (1990), 'Wear-mechanism maps', Scripta Metallurgical et Materialia, Vol.24, pp 87-97.

[12]. R. Holm, "The frictional force over the real area of Contact", Wiss.Vereoff. Siemens Werken, Vol. 17 (4), 1938.

[13]. Kragelskii, I. V.: Friction and Wear. Butterworths, Inc., 1965.

[14]. G. Fleischer (1973), Energetische Methode der Bestimmung des VerschleiRes. Schtnierungsrechnik 4(9). pp. 269-74.

[15]. Dhingra A.K., "metal replacement by composite", JOM, Volume 38, No. 03, (1986): pp.17.

[16]. R. Mehrabian, R.G. Riek and M. C. Flemings, "preparation and casting of Metal Particulate Non-Metal Composites," Metall. Trans, Vol. 5A, 1974, pp 1899-1905.

[17]. Zmitrowicz, Alfred. "Wear Patterns and Laws of Wear – A Review." Journal of Theoretical and Applied Mechanics 44, 2. (2006): pp. 219-253. Print.

[18]. Ritter J. (1970), 25th Annual Technical Conference, Reinforced Plastics/Composites Division, SPI, Inc., 53, pp 486-489.

[19]. Shao-Yun Fu, Xi-Qiao Feng, Bernd Lauke, Yiu-Wing Mai (2008), "Effects of particle size, particle/matrix interface adhesion and particle loading on mechanical properties of particulate–polymer composites". Composites: Part B 39, pp 933–961.

[20]. Kinloch A.J., Young R.J. (1983), Fracture Behaviour of Polymers, Chapman & Hall, London.

[21]. Sahu S. and Broutman L.J. (1972), Mechanical properties of particulate composites, Polymer Engineering and Science, 12(2), pp 91-100.

[22]. Mallick P.K. and Broutman L.J. (1975), Mechanical and Fracture Behaviour of Glass bead Filled Epoxy Composites, Materials Science and Engineering, 18(1), pp 63-73.

[23]. C. Swetha and Ravi Kumar (2011), Quasi-static uni-axial compression behaviour of hollow glass microspheres/epoxy based syntactic foams. Materials and Design 32 pp 4152–4163.

[24]. J.R.M. d' Almeida (1999), An analysis of the effect of diameters of glass microspheres on the mechanical behaviour of glass microsphere/epoxy matrix. Composite Science and Technology, 59, pp 2087-2091.

[25]. S. Basavarajappa and S. Ellangovan (2012), Dry sliding wear characteristics of glass-epoxy composite filled with silicon carbide and graphite particles. Wear, 296, pp 491–496.

[26]. K.C. Yung, B.L. Zhu, T.M. Yue and C.S. Xie (2009), Preparation and properties of hollow glass microsphere-filled epoxy-matrix composite. Composites Science and Technology, 69, pp 260–264.

[27]. Park Soo-Jin, Jin Fan-Long, Lee Changjin (2005), Preparation and physical properties of hollow glass microspheres-reinforced epoxy matrix resins, Material Science and Engineering A, 402, pp 335-340.

[28]. Ho Sung Kim and Mohammad Azhar Khamis (2001), Fracture and Impact behaviour of hollow micro-sphere/epoxy resin composites. Composite part A 32, pp 1311-1317.

[29]. Yan Hu, Riguo Mei, Zhenguo An and Jingjie Zhang (2013), Silicon rubber/hollow glass microsphere composites: Influence of broken hollow glass microsphere on mechanical and thermal insulation property. Composites Science and Technology 79, pp 64–69.

[30]. Jiwei Li, Xuegang Luo and Xiaoyan Lin (2013), Preparation and characterization of hollow glass microsphere reinforced poly (butylenes succinate) composites. Materials and Design 46, pp 902–909.

[31]. Ruoxuan Huang and Peifeng Li (2015), Elastic behaviour and failure mechanism in epoxy syntactic foams: The effect of glass microballoon volume fractions. Composites Part B 78, pp 401- 408.

[32]. Jinhe Wang, Guozheng Liang, Shaobo He, Lianli Yang (2010), Curing Behavior and Mechanical Properties of Hollow Glass Microsphere/Bisphenol A Dicyanate Ester Composites Journal of Applied Polymer Science, Vol. 118, pp 1252–1256.

[33]. Hyungu Im, Sang Chul Roh, and Chang Keun Kim (2011), Fabrication of Novel Polyurethane Elastomer Composites Containing Hollow Glass Microspheres and Their Underwater Applications. Ind. Eng. Chem. Res., 50 (12), pp 7305–7312.

[34]. P. Li, N. Petrinic, C.R. Siviour, R.Froud and J.M. Reed (2009), Strain rate dependent compressive properties of glass microballoon epoxy syntactic foams. Materials Science and Engineering A 515, pp 19–25.

[35]. Liang J.Z. (2005), Tensile and flexural properties of hollow glass bead filled ABS composites, Journal of Elastomers and Plastics, 37(4), pp 361–370.

[36]. Liang JZ. (2002), Tensile and impact properties of hollow glass bead filled PVC composites. Macromolecular Materials and Engineering, 287(9), pp 588–591.

[37]. Ferreira J.A.M., Capela C., Costa J.D. (2010), A study of the mechanical behaviour on fibre reinforced hollow microspheres hybrid composites, Composite ,41, pp 345-352.

[38]. C. Kanchanomai, N. Noraphaiphipaksa, Y. Mutoh (2011), Wear characteristic of epoxy resin filled with crushed-silica particles. Composites: Part B 42, pp 1446–1452.

[39]. M.Cirino, R.B.Pipes and K.Friedrich. "The Abrasive Wear Behaviour of Continuous Fibre Polymer Composites". Journal of Material Science, Vol 22, 1987, p. 2481.

[40]. A.P.Verma and P.C.Sharma, "Abrasive Wear Behaviour of GRP Composite, "The Journal of the Institute of Engineers (India), Pt MC2, Vol.72, March 1992, p 124.

[41]. S.R. Chauhan, Anoop Kumar, I. Singh (2010), Sliding friction and wear behaviour of vinylester and its composites under dry and water lubricated sliding conditions. Materials and Design 31, pp 2745–2751.